# **Model Inversion Attacks Meet Cryptographic Fuzzy Extractors**

Mallika Prabhakar\*, Louise Xu\*, and Prateek Saxena School of Computing, National University of Singapore {mallika, louisexu, prateeks}@comp.nus.edu.sg

Abstract—Model inversion attacks pose an open challenge to privacy-sensitive applications that use machine learning (ML) models. For example, face authentication systems use modern ML models to compute embedding vectors from face images of the enrolled users and store them. If leaked, inversion attacks can accurately reconstruct user faces from the leaked vectors. There is no systematic characterization of properties needed in an ideal defense against model inversion, even for the canonical example application of a face authentication system susceptible to data breaches, despite a decade of best-effort solutions.

In this paper, we formalize the desired properties of a provably strong defense against model inversion and connect it, for the first time, to the cryptographic concept of fuzzy extractors. We further show that existing fuzzy extractors are insecure for use in ML-based face authentication. We do so through a new model inversion attack called PIPE, which achieves a success rate of over 89% in most cases against prior schemes. We then propose L2FE-Hash, the first candidate fuzzy extractor which supports standard Euclidean distance comparators as needed in many ML-based applications, including face authentication. We formally characterize its computational security guarantees, even in the extreme threat model of full breach of stored secrets, and empirically show its usable accuracy in face authentication for practical face distributions. It offers attack-agnostic security without requiring any re-training of the ML model it protects. Empirically, it nullifies both prior stateof-the-art inversion attacks as well as our new PIPE attack.

# 1. Introduction

Machine learning (ML) systems are increasingly being used in security-sensitive applications, such as for authenticating users [1], [2], establishing content ownership [3], CSAM detection [3], and so on. In these applications, neural networks often encode security-sensitive inputs into vector representations called *embedding vectors*. For example, in face authentication, standard neural networks generate embeddings corresponding to a user's face image [1], [2]. These embedding vectors are stored on databases of application service providers [4] or on authentication devices [5].

Databases and devices storing sensitive information are frequently prone to breaches [6] and theft/loss [5] respectively. This gives rise to a threat model where the attacker gains access to *all information persistently stored* in the database or the device, as is typical of attacks colloquially

referred to "smash-and-grab" attacks. The breached information can be used to recover the original security-sensitive data corresponding to the embedding vectors, causing severe privacy risks. A well-known class of such attacks is called *model inversion*. Since their discovery in 2015 on deep networks [7], no defenses with strong formal security have yet been developed for model inversion attacks.

Model inversion attacks allow the adversary to recover inputs, given the outputs of the ML model. The canonical example introduced by the original work of Fredrikson et al. showcases the threat to face recognition systems, where outputs of deep networks can be used to recover the input face images reasonably accurately [7]. Over the last decade, ML models have evolved to serve tasks beyond classification which motivated the original work of Fredrikson et al. The outputs of modern ML models are embedding vectors which can be compared in  $\ell_2$  distance to other vectors. These vectors can be used to implement classification in a closedset [8], similarity testing in an open-set [2], [9], lookup in RAG databases [10], or generative tasks like text-to-image generation [11]. Recent works have shown that embedding vectors generated from today's ML models, if stored unprotected (in the clear), are highly susceptible to inversion attacks [12], [13], [14]. Therefore, it is important to devise a generic defense for model inversion attacks that works for applications where vector comparison with the standard Euclidean ( $\ell_2$ ) distance is used. In this paper, we will use the classical example of face recognition ML models, but our goal is to motivate a broader defense strategy.

Cryptographic post-processing defenses. One way to build a generic defense with provable guarantees is to turn to cryptographic methods. Specifically, can one post-process the output of the ML model with a cryptographic hash before they are stored, to create what we call protected embeddings, such that they can still be used for  $\ell_2$ -based authentication while resisting model inversion attacks? The advantage of post-processing defenses is that they do not require re-training of the ML model, and they are agnostic to any specific model inversion attack. They offer a complementary approach to many in-training defense methods [15], [16], [17], [18], which offer no formal security guarantees, nor do they aim to develop an attack-agnostic defense.

<sup>1.</sup> One could encrypt the embeddings with standard encryption. But, then the encryption key itself is persistently stored and offers no security when all persistent data is leaked.

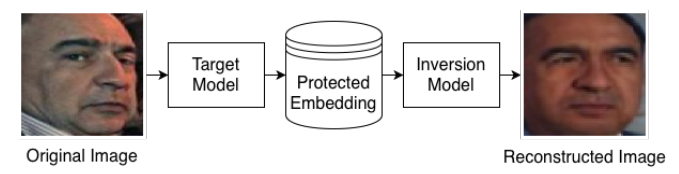


Figure 1: An example inverting the FacialFE-protected embedding vector to obtain a face image similar to the original using PIPE.

Remarkably, despite their appeal, post-processing defenses have not yet been considered for tackling model inversion.

To understand why, it is perhaps useful to draw parallels with how hashing protects against the same threat model of password database breaches [19]. It is standard practice to store passwords salted-and-hashed using standard cryptographic hash functions like SHA256, so that inversion of the plaintext passwords from a leaked password database becomes hard [20]. However, such hash functions do not work for protecting embeddings generated from ML models. This is because ML models are designed to tolerate noise: Embeddings generated from two different face images are considered to be of the same person if their generated embedding vectors are close in  $\ell_2$  distance. In face authentication, the user being authenticated must have an embedding vector that is close to the one expected, unlike passwords that must match exactly. However, standard cryptographic hash functions (eg. SHA256) used for salting-and-hashing passwords cannot tolerate any errors in inputs, i.e., even a single bit change in input induces a large change in output of the hash function. Hence, standard hash functions like SHA256 cannot be used to protect ML embedding vectors.

Post-processing defenses for tackling model inversion attacks on modern ML models have not been demonstrated so far. Nonetheless, there have been *partially-secure* post-processing candidates that one could leverage from prior literature as a starting point [21], [22]. These schemes allow noisy inputs to authenticate successfully as desired. Indeed, in our evaluation, we show that these schemes are effective against prior model inversion attacks which target unprotected embeddings [14], reducing their success rate from 99% to 2%. However, as we will show, prior protection schemes are still *breakable* and do not enjoy cryptographically strong properties that are ideally desired.

Our PIPE attack. To highlight the gap between the ideal security properties desired and that offered by partially-secure post-processing schemes, we first present a new adaptive attack called PIPE<sup>2</sup>. PIPE is a model inversion attack that targets vector embeddings generated using ML models for face images, and post-processed with prior protection mechanisms. Briefly, PIPE recovers a surrogate embedding vector from the protected embedding, then leverages a separate inversion model to recover images close to the original input image. It assumes *full leakage*—the adversary gets access to all the information stored persistently on a database, including protected embedding vectors. The attack only

2. PIPE stands for 'Post-leakage Inversion of Protected Embeddings'

needs *black-box* query access to the target ML model and public datasets characterizing the input (face) distribution, but no knowledge of the training dataset of the target model.

We evaluate our PIPE attack against two of the most potent partial protection mechanisms we know of: Facial-Fuzzy Extractor (Facial-FE) [23] and Multispace Random Projection (MRP) [24]. PIPE highlights the weaknesses of these constructions when applied to face authentication under the realistic threat model of full data leakage. Experimentally, PIPE has attack success rate of over 47% for embeddings generated from state-of-the-art models like Facenet [2] and ArcFace [1] against both of these partial defenses (see Tables 3 and 4). In most settings, the observed attack success rate is well over 89%.

Figure 1 shows a successfully recovered face from Facial-FE-protected embeddings using PIPE for a quick illustration. It is close to the original image both visually and as per image similarity metrics like LPIPS [9], showing the privacy-invasive nature of the attack. The normalised embeddings of these images are also close in  $\ell_2$  distance.

Towards an ideal defense. Does there exist a cryptographic primitive for  $\ell_2$ -based authentication that would *provably defeat all model inversion* attacks, regardless of the underlying ML model, with the full-leakage threat model? Three properties would be required by such a primitive: noise tolerance, security under full leakage, and utility. One can think of it as an analogue to the salt-and-hash mechanism used for passwords, except that this primitive must tolerate noise in the input vector. Additionally, it should be hard to recover an input close to the original input even when given all outputs. We introduce this ideal primitive in Section 3 and present its formal definition in Appendix A.

As a key conceptual contribution (see Theorem 2), we show that the ideal primitive can be achieved if one constructs a secure fuzzy extractor—a cryptographic construct [25] that predates model inversion attacks by a decade—for the desired  $\ell_2$  norm vector comparison. Finally, as a technical contribution, we propose a candidate construction called the L2FE-Hash, a lattice-based fuzzy extractor (FE) that enables  $\ell_2$  norm vector comparison on hashed outputs. We formally show that it is computationally secure under certain assumptions on the input distribution (see Theorem 1). We empirically show that it has reasonable accuracy for face authentication with state-of-the-art ML models. We also confirm that L2FE-Hash resists prominent prior model inversion attacks as well as our adaptive PIPE attack in our experimental evaluation (see Section 8).

To the best of our knowledge, ours is the first work to provide a  $\ell_2$ -based FE with strong practical security and retain reasonable accuracy on real-world face distributions.

Generalizing beyond faces. While we have chosen the face authentication system as a concrete application, aligning with the original work on model inversion [7], the threat of inversion attacks on embedding vectors extends well beyond that. All our security properties, attacks, and definitions are generic—they are defined abstractly for models that produce similar high-dimensional embedding vectors

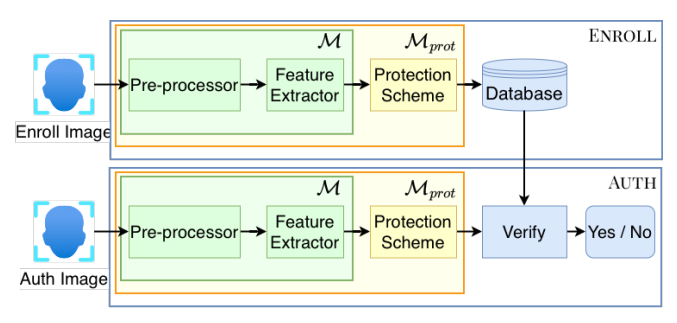


Figure 2: A face authentication system with ENROLL and AUTH functions.  $\mathcal{M}$  represents models that output unprotected embeddings and  $\mathcal{M}_{prot}$  represents the models with post-processing protection mechanisms that output protected embeddings.

for similar inputs. We define closeness with respect to  $\ell_2$  distance since it is common in face authentication, but one can easily extend our definitions to any distance metric. One can readily consider modalities that rely on  $\ell_2$  distance, like audio and text [26], [27] in future work. Likewise, one can consider other security applications such as image similarity checking for copyright infringement or CSAM detection [3].

Contributions. To the best of our knowledge, this is the first work that connects two long-standing but disparate lines of research, namely on model inversion attacks and on cryptographic fuzzy extractors. First, we show a new model inversion attack called PIPE which reliably defeats existing post-processing mechanisms, highlighting the lack of practical defenses with desirable cryptographic properties. Second, we describe a candidate fulfilling all ideal properties practically, called L2FE-Hash. We prove that fuzzy extractors are robust against inversion attacks generically, and show that L2FE-Hash is an  $\ell_2$ -norm fuzzy extractor construction that is empirically robust against PIPE, while having a usable accuracy for face authentication systems.

# 2. The Problem

Protecting long-term secrets, like authentication credentials, is an important goal in the event of catastrophic data breaches. We explain how this problem manifests in the context of vector embeddings used in modern ML models for face authentication, following the inspiration set in [7].

#### 2.1. Application: ML Face Authentication

Billions of users have had password credentials leaked via data breaches, posing serious threats to security and privacy. As authentication services, for example ML-based face authentication like ClearView [4] and crypto wallets [5] store credentials (embeddings) derived from face images persistently, they face a similar risk from breach or theft [6].

A typical face authentication system employs two phases: enrollment and authentication, denoted by two functions ENROLL and AUTH respectively (see Figure 2). During enrollment, the user provides an image to the authentication

system. The authentication system calls the ENROLL function on an image to extract a vector embedding. Specifically, the ENROLL function uses an ML model  $\mathcal M$  often called a "feature extractor" which generates a representative embedding vector  $x \in \mathbb R^m$  for a given input image I. It then stores this embedding vector x in the database along with the username. When a user later tries to log into the system, it calls the AUTH function using its face image I', possibly different from I. AUTH uses  $\mathcal M$  to generate an embedding x' from the given input I', and retrieves x from the database using the username. If I and I' are similar, i.e. different images of the same face,  $\mathcal M$  produces vectors x and x' that are close (say in the standard  $\ell_2$  distance). So, AUTH compares the newly computed x' with the retrieved x and accepts the authentication request iff the two are close.

In summary, the authentication server stores a high-dimensional *embedding vector* x in the database. It expects that a legitimate user will have face images that  $\mathcal{M}$  maps to vectors close to x. It is equally important for security that an illegitimate user will not be able to present an input image at the time of authentication that  $\mathcal{M}$  maps to vectors close to x. Modern neural networks and generative AI models generate embedding vectors in various practical ways that satisfy both these properties, with acceptably low error rates, and thus are increasingly being used in production systems.

# 2.2. Inversion of Unprotected ML Embeddings

Consider an attacker who gets unauthorized access to the database storing sensitive embedding vectors persistently. If no protection mechanism was implemented (i.e.  $\mathcal{M}$  outputs were stored directly in Figure 2), then the "unprotected" embedding x retains significant information about the original image, and there is a risk that the original image can be inverted from x approximately. Recent prior works have shown that ML models can be trained [12], [13], [14] to perform such inversion for standard face recognition ML systems ( $\mathcal{M}$ ) such as Facenet [2] and ArcFace [1]. If successful, the inverted image is close enough to the original face image that it passes authentication with  $\mathcal{M}$ . Prior works have reported attack success rates of over 90% (see Section 6 too). Thus, highly effective inversion attacks on unprotected embeddings are known, posing a serious privacy risk.

## 2.3. Protecting Embeddings via Post-processing

A good defense mechanism should protect embedding vectors derived from sensitive inputs when they are persistently stored. Ideally, the defense should not be attack-specific and should generically defeat all feasible attacks. Moreover, we are not seeking solutions for securing persistent database storage via additional trust in hardware [28] or in third parties to securely store cryptographic keys.

A promising approach to such a defense is via postprocessing methods applied directly on embeddings generated from any trained ML model. They can be easily integrated into the face authentication pipeline by replacing  $\mathcal{M}$  with  $\mathcal{M}_{prot}$  shown in Figure 2. We focus on **post-processing protection schemes** in the paper since they can be directly implemented on current models without re-training. Such post-processing defenses exist in prior cryptographic literature. We visit two most prominent such mechanisms in Section 4, which our attack will target.

Many prior defenses are not in the post-processing regime. They are methods that work during model training to reduce the amount of sensitive information held by the resulting embeddings [15], [16], [17], [18]. But such mechanisms have had limited success. Recent works show that the defended model remains susceptible to prior inversion attacks, with  $\geq 30\%$  users being re-identified for models that have accuracy  $\geq 80\%$  [15], [17], [29]. Therefore, we leave this alternative line of mechanisms out of scope. Besides, they are complementary to post-processing mechanisms.

## 2.4. Threat Model

We focus on inversion attacks on *protected embeddings*, i.e., embeddings that have been post-processed before being stored. We assume the *full-leakage* threat model, much the same as what password hashing is meant to protect against. We assume that all *persistently stored* metadata is leaked all at once, including any randomness that is strictly necessary for the legitimate authentication to work. Therefore, the adversary's goal is as follows: Given any leaked face embedding computed as the output of ENROLL, along with requisite randomness, reconstruct an image that resembles the original image. Note that ephemeral data such as (I, I', x') used during ENROLL and AUTH is not stored persistently and the attacker does not have access to it.

To keep attack assumptions minimal, we work in the black-box threat model. We adapt the black-box model presented in [7] and assume the attacker only has query (or API) access to the target model  $\mathcal{M}_{prot}$  (see Figure 2). The query exposes protected embeddings, instead of classification results as presumed in [7] for generality, since ML models today are used in non-classification tasks too. Moreover, protection schemes used by the target models are publicly available algorithms known to the attacker.

We assume that the attacker has access to a public dataset of face images, similar to that assumed in the original attack [7]. Our public dataset does not overlap with the leaked database, and the attacker can query  $\mathcal{M}_{prot}$  on this dataset to obtain corresponding embeddings. These assumptions are practical and common to prior attacks [14], [30], [31]. This is also analogous to how password crackers use real-world password distributions gleaned from leaked password databases [19], [32].

## 3. An Ideal Post-Processing Primitive

The need for post-processing protection mechanisms has been recognized in prior cryptographic literature [21], [22], but their desired security properties have not been carefully established in the context of model inversion. In particular,

**Algorithm 1** Enrollment and Authentication with ideal primitive.

```
1: procedure ENROLL(I, \mathcal{M})
         x := \mathcal{M}(I)
                                                                         \triangleright x \in \mathbb{R}^n
                                                              \triangleright y \in \mathbb{R}^m, s \leftarrow S
3:
         (y,s) := GEN(x)
         Persistently store (y, s) in Database
4:
5: end procedure
1: procedure AUTH(I', \mathcal{M})
                                                                        \triangleright x' \in \mathbb{R}^n
         x' := \mathcal{M}(I')
3:
         Load (y, s) from Database
4:
         y' := REP(x', s)
         Return VERIFY(y', y)
6: end procedure
```

no secure mechanisms from prior works satisfy the desired properties, as we will experimentally show in Section 6.

# 3.1. Desired Properties

To systematically characterize the problem, we define the properties an ideal protection primitive should satisfy. We do so informally here and provide formal definitions in Appendix A. The ideal primitive contains two subroutines: GEN and REP. GEN takes input embedding x and outputs a protected embedding y with auxiliary random seed s. The function REP takes some close input x' and helper s to produce y'. An ideal primitive must satisfy 3 properties:

- 1) Correctness (Noise tolerance): For close inputs x and x', when x is enrolled, x' should authenticate successfully with high probability. In other words, for GEN(x) = (y, s), the reproduced embedding REP(x', s) = y' is equal to y with high probability.
- 2) Security (Fuzzy One-wayness): Given outputs (y, s) := GEN(x), finding any input x' close to x is hard.
- 3) Utility: The entropy of the output embeddings y, conditioned on helper s, should be comparable to that of the input embeddings x.

Authentication based on the ideal primitive. If such a primitive exists, Algo. 1 shows how it readily works with a face authentication system. The ENROLL function receives an enrollment image, applies GEN to the image's embedding vector x, then stores the corresponding protected embedding y in the database persistently. The AUTH function receives an authentication image, and checks if it has matching identity with the enrollment image. Specifically, it uses REP to compute some y' using x'. The VERIFY function compares y' with the stored y, and outputs Accept only if y' = y. The user is allowed to log in only if VERIFY returns Accept.

Why these properties? The noise-tolerance Prop. 1 ensures that protected embeddings can be readily used in security applications that demand  $\ell_2$ -based closeness comparison. For example, in a face authentication system,  $\mathcal{M}$  generates unprotected embeddings close in  $\ell_2$  norm given similar face images. After applying the protection scheme, these embeddings should map to the same protected vector allowing AUTH to perform exact comparison with high accuracy.

The recovery of an unprotected embedding close to the original poses a high privacy risk, as prior work has shown

TABLE 1: Symbols used in this paper with definitions

Symbol	Definition
$\mathcal{M}$	Target (feature extractor) model
$\mathcal{M}_{prot}$	Target model with post-processing protection
I	Input image obtained during enrollment
I'	Input image obtained during authentication
$\overline{x}$	Input vector computed during enrollment
x'	Input vector computed during authentication
$x^*$	Surrogate vector recovered from y
$\overline{y}$	Output protected vector obtained from $x$ (persistent)
y'	Output protected vector obtained from $x'$
$\overline{m}$	Size of vector x
$\overline{n}$	Size of vector y
l	Size of ephemeral vector b in L2FE-Hash (Algo. 3)
t	Closeness $\ell_2$ -threshold between $x$ and $x'$
T	Closeness $\ell_2$ -threshold between $y$ and $y'$
s	Random seed vector (persistent)
λ	Security parameter which controls size of seed s
ζ	Entropy of input distribution

that unprotected embeddings can be inverted back into original images. Prop. 2 ensures that the embedding x is hard to recover, even approximately within a distance t, even if we leak the auxiliary seed s and the stored output y. So, Prop. 2 generically defeats inversion attacks under the full-leakage threat model—the protected embedding cryptographically hides the unprotected embedding it is generated from.

Prop. 3 is necessary to prevent trivial functions that compress inputs into a very small output domain. If output entropy is too small, the adversary would be able to guess inputs by brute-forcing. Moreover, it would render the primitive useless in applications that want to use the output to distinguish various inputs. For example, a primitive designed for face authentication should map input embeddings corresponding to different users to different protected embeddings. Hence, the output entropy required for Prop. 3 depends on the application use case and is often related to the input entropy. We use the standard computational HILL entropy here, please see Definition 3 in Appendix A.

## 3.2. Relation to Fuzzy Extractors

We will later show formally that the desired properties are achieved by a fuzzy extractor. Briefly, the GEN and REP subroutines of a fuzzy extractor work similarly to the GEN and REP subroutines of our ideal primitive, albeit with different security formulations. However, existing fuzzy extractor constructions are designed for  $\ell_0$  distances, such as the Hamming distance or set difference, to suit the use case of iris or fingerprint authentication [25]. There is no secure construction of an  $\ell_2$ -based fuzzy extractor, as needed for practical use with face distributions yet. We address this gap by proposing an ideal primitive for an  $\ell_2$ -based authentication system, and give a working candidate construction L2FE-Hash of the ideal primitive in Section 7.

# 4. Existing Protection Schemes

As a starting point for post-processing defenses, one can consider two cryptographic schemes that are state-of-theart of their respective family of concepts: a Facial-Fuzzy Extractor and Multispace Random Projection. We detail their constructions and explain why they only partially-secure under the threat model of full leakage. They serve as two main targets for our new attack PIPE presented in Section 5, and experimentally confirm it in Section 6.

# 4.1. Existing Scheme via Fuzzy Extractor

A fuzzy extractor (FE) is an existing cryptographic primitive that derives high-entropy cryptographic keys from a noisy input source, such as human biometrics [25]. Specifically, it extracts a uniformly random string from an input vector, such that the same string can be reliably reproduced from other close input vectors. This "error-correcting" property makes FE well-suited for noisy-source authentication.

**Background on FE.** A FE primitive is defined by two functions GEN and REP. The function GEN takes input x and outputs a secret extracted key r and a public helper string p. The function REP takes some close input x' and helper p to reproduce r. Typically, an FE scheme is instantiated using another cryptographic primitive called a secure sketch, which provides the error-correction property, and a randomness extractor, which ensures uniformity of the secret r [25]. The security property of FE guarantees that the helper p can be released publicly without revealing any information about r, enabling r to be used as a secret key for any downstream cryptographic applications.

**FE-based Authentication.** The roles of the FE GEN outputs r and p as secrets and helpers respectively correspond to the outputs y and s of the ideal primitive we defined earlier. Hence, an FE scheme can be easily integrated into the face authentication pipeline in Algo. 1 by substituting with FE's GEN and REP functions  $^3$ . Note that only (r,p) must be persistently stored for subsequent use at authentication time.

No secure FE construction prior to our work that performs  $\ell_2$  norm error-correction is known to the best of our knowledge. To illustrate the lack of such a primitive, we will take the closest FE scheme we know of that approximates for  $\ell_2$ -correction, called Facial-Fuzzy Extractor (or Facial-FE) [23], and show that it is insecure.

**Facial-FE.** Facial-FE claims to provide the only computationally secure FE that works for an approximation of the  $\ell_2$  metric using a specific lattice-based metric [23]. It uses dense and efficiently decodable lattices, where each input is decoded to a lattice point, and the difference vector is the helper string. The hashed input and the public helper string are stored as the persistent secret to help reconstruct the original input from the authentication input.

<sup>3.</sup> Other methods of integrating FE into face authentication have also been proposed, such as [33] using the FE secret output r to generate keys for a public-key encryption scheme, though this distinction is not relevant.

Algorithm 2 Facial-FE construction from [23] Algo. 1, 2, 5, 6.

```
1: procedure GEN
          \begin{array}{l} \text{Input: } x \xleftarrow{\mathcal{X}} X \\ k \leftarrow \{0,1\}^{\lambda-m} \end{array}
                                                                                     \triangleright x \in \mathbb{R}^m
2:
3:
4:
          c := \operatorname{Decode}(x)
                                                                                      \triangleright c \in \mathbb{Z}^m
          ss := c - x
5:
                                                                                      \triangleright p \in \mathbb{Z}^{\lambda}
          p := (ss, k) and r := H_k(x, ss)
          return (r, p)
                                                        \triangleright r, p are stored persistently
7:
8: end procedure
1: procedure REP
          Input: (x', p)
2:
          Parse p as (ss, k)
3:
          c' := x' + ss
4:
          c^* := \text{Decode}(c')
                                                             Decode is E8-decoder
5:
          \tilde{x} := c^* - ss
6:
          return H_k(\tilde{x}, ss)
7:
8: end procedure
```

The Facial-FE construction from [23] using the E8-lattice decoder as the Decode sub-algorithm is reproduced as-is in Algo. 2, adapted to use symbols consistent with our work.  $H_k$  denotes a cryptographic hash with a random key k.

**Facial-FE is not ideal.** Facial-FE can satisfy Prop. 1 because the linearity of lattices allows for correction of errors within the Voronoi cell, which is an approximation for correction of errors within some  $\ell_2$  distance. However, it does not satisfy the security property Prop. 2. Notably, it releases a public helper string p, which contains a string ss (called a secure sketch output). The key issue is that the construction uses a *deterministic* decoder, i.e., there is no randomization in producing ss. Since c is determined by s for a fixed lattice, ss = c - s can reveal a lot of information about s. Our attacks in Section 5 take advantage of this weakness and use ss to find an s close to s.

# 4.2. Existing Scheme via Random Projection

Another popularly used primitive for protecting embeddings via post-processing is multispace random projection (MRP) [24]. There are many projection-based schemes used to protect biometrics, but they are variants of the common MRP building block [34], [35]. MRP works by projecting input vectors onto a random subspace of lower dimensionality, determined by a user-specific random seed. Then it can perform vector comparisons for authentication in the projected vector space without storing the original vectors.

**Background on MRP.** MRP is a randomized technique that projects the input vector along random vectors, first proposed by [24]. MRP samples a random Gaussian matrix  $R \in \mathbb{R}^{n \times m}$  where each entry is from the standard normal distribution with mean 0 and standard deviation 1. Each row vector in R thus has a random vector direction in the Euclidean space. It projects the input vector  $x \in \mathbb{R}^m$  to output vector  $y \in \mathbb{R}^n$ , where n < m, as follows:

$$y := f(x) = \frac{1}{\sqrt{n}}Rx\tag{1}$$

The coordinates of y are thus the projections of x along the row vectors in R. MRP assumes that R is stored securely in a database and never leaked. We refer to this threat model as  $partial\ leakage$ . In typical breaches, however, everything stored on the server or device is leaked. The security offered by MRP schemes is not formally defined or critically analyzed in the full-leakage threat model so far.

MRP-based Authentication. One can use MRP in Algo. 1 by setting s=R and y as shown in Eqn (1). Instead of using exact matching as the VERIFY function, MRP-based face authentication uses closeness matching, where VERIFY will accept as long as (y,y') are close within some threshold distance. Thus, if the unprotected embedding x at the time of enrollment is close to the x' presented during authentication within distance t, then the corresponding protected embeddings y and y' should be close to each other within distance T. If so, then the MRP scheme serves the desired functionality of correctness. Note that both y and the random matrix R are stored persistently in the database.

**MRP** is not ideal. MRP is not an ideal primitive because it does not satisfy Prop. 2. It only satisfies the much weaker non-invertibility property, stated informally below:

Given s and y, it is hard to find x exactly.

MRP is non-invertible because Rx=y gives us a set of under-determined linear equations. However, non-invertibility does not preclude approximate recovery, i.e., finding an input vector x' within distance t from x. Thus, it is a weaker security property than Prop. 2. We show attacks against MRP in Section 5 that exploit this distinction.

MRP does meet  $\ell_2$  norm correctness Prop. 1 because of the phenomenon captured by the Johnson-Lindenstrauss (JL) Lemma [36], [37]. The JL Lemma 1 given below ensures that the pairwise distance between all points in a set of k points is maintained within an arbitrarily small factor by random projection maps. In other words, the projected data still retains enough information for authentication to work.

**Lemma 1** (Johnson–Lindenstrauss Lemma [37] rephrased). For any  $0 < \epsilon < 1$  and any integer k > 0, let n be a positive integer such that  $n \ge \frac{4 \ln k}{\epsilon^2 / 2 - \epsilon^3 / 3}$ . Then for any set S of k = |S| data points in  $\mathbb{R}^m$  and the randomized map  $f: \mathbb{R}^m \to \mathbb{R}^n$  given in Eqn (1), with high probability for all  $x_i, x_j \in S$ :

$$(1-\epsilon)\|x_i-x_i\|_2^2 \le \|f(x_i)-f(x_i)\|_2^2 \le (1+\epsilon)\|x_i-x_i\|_2^2$$

The JL Lemma tells us how, with an appropriate choice of n, MRP can satisfy correctness (noise-tolerance) Prop. 1. Specifically from the lemma, it can be seen that if the dimensions of the projected space  $n=O(\ln k/\epsilon^2)$ , then the distance between any two vectors out of k is maintained with a reasonably small  $\epsilon$  multiplicative factor of the original distance in n dimensions. This can be used to select the distance threshold T to use for verification, as it is a function of projected dimensionality n, the noise tolerance (distance) of unprotected embeddings t, and the total number of users k. The tunable constant  $\epsilon$  determines n and reliability  $\delta$ .

We conjecture that an MRP can also satisfy Prop. 3 since random projections largely transfer the entropy of the input to the output—they do not create too many collisions.

#### 5. The PIPE Attack

We propose a new model inversion attack called PIPE to highlight the gap between existing candidates available from literature and the ideal defense. Our evaluation using PIPE against existing schemes is in Section 6. It confirms the gap experimentally. We will also evaluate newly proposed L2FE-Hash in Section 8 to show the security improvement.

# 5.1. Attack Setup

As discussed in Section 2, the attacker has black-box query (API) access to the target model  $\mathcal{M}$  and a public face dataset. It knows the protection mechanism used by  $\mathcal{M}$ . No ephemeral secrets or intermediate values computed in Algo. 1 are persistently stored or leaked to the adversary; only the protected embedding vectors y and the corresponding seed s are. For FE-based schemes, the protected embedding y is the extracted key r and the seed s is the public helper p. For MRP, the protected embedding y is the projected vector y and the seed s is the projection matrix R. All persistently stored data is leaked to the adversary.

**Choice of seed.** We consider the attack setup where the seed s is a different value per-user. The use of different seeds is similar to how passwords of each user are hashed with different salt values, which in the context of password hashing, is expected to increase the attacker's effort per user. It has been considered in prior works on protecting embeddings as well. For example, the MRP seed is referred to as a "user-specific PRN" [24], and the Facial-FE seed includes a user-specific deterministic vector ss.

# 5.2. Attack algorithm

There are two parts in the PIPE attack. Step 1 is to recover a surrogate embedding from all available information. This step demonstrates the weakness of current protection schemes in the full-leakage setting. Step 2 is to perform inversion on the surrogate embedding to obtain the original image. We train a diffusion model conditioned on these surrogate embeddings to reconstruct original images.

#### 5.2.1. Step 1: Recovering surrogate embedding

The step aims to recover a surrogate vector  $x^*$  from y and s, such that  $x^*$  contains information about the original x which was used to generate y. This step is specific to the protection scheme since the attacker can utilize knowledge about the scheme to devise the attack.

PIPE **Step 1 for Facial-FE.** Facial-FE outputs (p, r) where p = (ss, k) and  $r = H_k(x, ss)$ , see Algo. 2. Since r is a random value, we attack only using the public ss which persists in the database. Recall from Section 4.1

that ss=c-x and both c and x are determined by x due to the use of a deterministic lattice. We exploit this weakness. Specifically, we observe that decoded codeword c is a deterministic sparse vector for each x, making ss largely resemble the input x. Hence the surrogate vector  $x^*=ss$ . Our successful attack implies that Facial-FE does not even satisfy standard security properties of fuzzy extractors.

PIPE **Step 1 for MRP.** In the case of MRP, the attacker wants to recover some  $x^*$  from y=Rx. Since  $R\in\mathbb{R}^{n\times m}$  and n< m, R is a compression map. Solving  $x=R^{-1}y$  is an under-determined system of linear equations, so Gaussian elimination is not usable directly. To resolve this problem, we propose to compute a Moore-Penrose inverse [38] or simply, pseudo-inverse of R, denoted as  $R^\dagger\in\mathbb{R}^{m\times n}$  using the singular values of R. The matrix  $R^\dagger$  thus obtained is a right pseudo-inverse of R as m< n. By left multiplying  $R^\dagger$  to the leaked vector y, we get an m-dimensional vector  $x^*$ .

$$R^{\dagger}y = R^{\dagger}Rx = x^*$$

Since we are using a right pseudo-inverse for left matrix multiplication, we do not have the guarantee that  $x^*$  is equal to or close to x. However, we expect that  $x^*$  contains information similar to the original x since the pseudo-inverse uses the n singular values of R, carrying most of the information about how R compresses  $x \in \mathbb{R}^m$  to  $y \in \mathbb{R}^n$ .

## 5.2.2. Step 2: Inverting embedding

Next, we want to invert  $x^*$  obtained from the previous step to get an image close to the original image I. It is generally difficult to invert  $\mathcal M$  just by knowing a random value y, but thanks to Step 1, we have recovered  $x^*$  that is significantly correlated to the input x. Step 2 uses  $x^*$  as an input to an *inversion model* to recover I'.

There are many existing ML models that can be considered for use as inversion models. Most create good quality images but dissimilar images [12], or poor quality but representative images [14], [39]. Moreover, these models have only been examined in the setting of image inversion from "unprotected" embeddings x and not from approximately recovered  $x^*$  as needed in our attack. For our inversion model, we adapt the classifier-guided diffusion model by [40] and use surrogate vectors  $x^*$  obtained in Step 1 instead of class labels as the guidance vector. The public face datasets are used to train the model to learn an association between the distribution of face images I and surrogate embeddings  $x^*$ . Once trained, the inversion model is fixed for use in attacks. At attack time (post-training), the inversion model then generates images by conditioning on the surrogate  $x^*$ recovered by Step 1 from the leaked embedding x.

**Defining Attack Success.** We consider all evaluated inversion attacks successful only if they recover an image close to that which the user originally enrolled with. That is, if the  $\ell_2$  distance between two normalized (unprotected) embedding vectors output by  $\mathcal{M}$  for the original and inverted image is less than a threshold t, denoted below as  $\approx_t$ . The  $\ell_2$  norm is

a commonly used<sup>4</sup> training loss for face recognition models. We define *attack success rate* (ASR) as:

 $\frac{\#(\mathcal{M}(\text{inverted image}) \approx_t \mathcal{M}(\text{original image}))}{\#\text{test images}}$ 

# 6. Experimental Evaluation: Existing Defenses

We evaluate partial protection schemes applied to stateof-the-art feature extractor models. Section 6.2 reports the effectiveness of PIPE and contrasts it to that of random guessing. Section 6.3 reports on the potency of prior attacks.

# 6.1. Methodology & Attack Setup

Models. We use two pre-trained state-of-the-art feature extractor models  $(\mathcal{M})$  for face images, Facenet [2] and Arcface [1], loaded through the DeepFace library [41]. They are pretrained on VGG-Face2 dataset [42] and Casia-Webface [43] dataset respectively. They are often used in works on inversion attacks targeting unprotected embeddings [13], [14] and achieve high accuracy. Before passing the image to the feature extractor, we pre-process the image using MTCNN [44]. Table 2 summarizes details of these models used to extract faces from input images. The true positive rate (TPR) of these models, as seen in Table 2, is over 79.3% with Facenet having a larger TPR of 89.5% with a 0.8% false positive rate (FPR) which suffices for reliable authentication. These values are computed on 1000 same users image pairs and 1000 different users image pairs over the Celeb-A dataset [45]. The thresholds were determined for  $\ell_2$  distance of normalised embeddings using the chefboost implementation of the decision tree algorithm [46].

We augment the feature extractor model  $\mathcal{M}$  with an additional post-processing layer of protection scheme that produces protected embeddings. We refer to this model as the *target model*. The model  $\mathcal{M}$  itself remains unchanged. The same feature extractor model  $\mathcal{M}$  is used to determine the attack success rate of the reconstructed images.

**Training of Inversion Models.** Recall that PIPE uses an embedding conditioned diffusion model adapted from the implementation by [40] as the inversion model in PIPE attack. We use hyperparameters and image size of  $64 \times 64$  as recommended in [40], with a learning rate of 1e - 4, batch\_size =64, ema\_rate of 0.9999 and anneal\_steps 25000.

**Datasets & Ensuring no overlaps.** To illustrate that our attack can work across multiple datasets and face distributions, we use 3 image datasets: Casia-Webface [43], Celeb-A [45], LFW [47]. We perform *cross-dataset evaluation*. Specifically, the inversion model used in PIPE is trained only on the Celeb-A dataset, while the ASR is reported for all the 3 datasets separately. Furthermore, the inversion model is tested on 1000 different users (images) in all 3 datasets,

but trained only on 9177 user images in the Celeb-A dataset different from the ones tested on. Thus, there is no overlap in identities used in training set of PIPE and those tested.

Distance Thresholds. To calculate ASR, we first compute the thresholds t by evaluating the distance between 1000 pairs of images of the same user and 1000 pairs of images of different users, given in Table 2. The ASR evaluation is performed by comparing the distance of unprotected embeddings with respect to t, rather than comparing protected embeddings. This is a sound evaluation step since all protection schemes MRP and Facial-FE guarantee that close inputs (unprotected) have corresponding outputs be close. Recall that for MRP, the VERIFY function should output ACCEPT if the distance between protected embeddings is below some threshold, i.e.  $d(y, y') \leq T$ . Nonetheless, by JL Lemma, this is equivalent to  $d(x, x') \leq t$ . Similarly, for Facial-FE and L2FE-Hash, the VERIFY function should output ACCEPT if protected embeddings match exactly for the original and inverted images. This only happens when the unprotected embeddings are close in  $\ell_2$  norm i.e.  $d(x, x') \leq t$ .

All experiments are performed on NVIDIA A40 GPUs. The inversion model in PIPE takes around 10 hours to train for CelebA, requiring 25,000 anneal steps in diffusion.

**Random Guessing.** Before analyzing PIPE results at face value, we need to see the advantage of an attacker who guesses randomly. If there are 1000 possible identities for an embedding, one might naively expect an ASR for random guessing to be 1/1000 = 0.1%. Practically though, feature extractors on natural distributions have false positives and false negatives, leading to a higher ASR. To evaluate ASR of random guessing, we take 1000 images, each belonging to a different user, and measure how many unprotected embeddings fall within  $\ell_2$  distance t of the chosen embedding. We repeat this procedure 1000 times for all three datasets as well as the two feature extractors. ASR for random guessing is reported in all cross-dataset experimental Tables 3 and 4 and later in Table 10, which are about 1% to 8% on average.

# 6.2. PIPE Against Existing Protection Schemes

We run PIPE against embeddings protected with Facial-FE and MRP. Our results presented here are for the cross-dataset evaluation while using different seeds per user.

PIPE **Against Facial-FE.** Table 3 shows that PIPE succeeds with a high ASR. When setting up Facial-FE, we configured its parameters to attain  $\leq 70\%$  FNR<sup>5</sup> as specified by [23]. This requires the face vectors to be scaled down. The scales we obtain for Facenet and Arcface embeddings are 5.7 and 1.39 respectively. At this scale, which is required for reasonable accuracy, we notice that the inputs tend to decode to lattice points c that are sparse 512-dimensional vectors with more than 194 zero elements. Consequently, the helper string ss=c-x contains significant information about s making Facial-FE insecure . This issue cannot be

<sup>4.</sup> Another commonly used metric is cosine similarity. For normalised embeddings u and v, cosine similarity  $\cos\theta$  is directly related to the  $\ell_2$  norm since  $\|u-v\|_2^2=2-2\cos\theta$ . The angle between u and v is  $\theta$ .

TABLE 2: The table provides details for the chosen feature extractor models. The threshold (t), True positive rate (TPR), and false positive rate (FPR) are computed over 1000 same and 1000 different identity pairs from Celeb-A dataset.

Model	Pre-processor	Input image size	Output vector size	Distance metric	Threshold (t)	TPR %	FPR %
Facenet	MTCNN	160x160	512	Euclidean normalised	1.103	89.5	0.8
ArcFace	MTCNN	112x112	512	Euclidean normalised	1.101	79.3	7.4

TABLE 3: Cross-Dataset ASR (in %) of PIPE attack against Facial-FE-protected embeddings and Success Probability of Random Guessing ( $\pm$  standard deviation).Training set is Celeb-A.

Test set	Model	PIPE %	Random %
Celeb-A	Facenet	100.0	$1.01 \pm 0.52$ $1.25 \pm 0.7$ $1.33 \pm 0.71$
LFW	Facenet	99.5	
CASIA	Facenet	99.6	
Celeb-A	ArcFace	95.8	$8.19 \pm 9.13$
LFW	ArcFace	96.2	$1.46 \pm 1.33$
CASIA	ArcFace	89	$1.57 \pm 2.81$

TABLE 4: Cross-Dataset ASR (in %) of PIPE in full leakage (PIPE), partial leakage (Partial) and Success Probability of Random Guessing (± standard deviation) against MRP-protected embeddings. Training set is Celeb-A.

Test set	Model	PIPE %	Partial %	Random %
Celeb-A	Facenet	99.4	0.9	$1.01 \pm 0.52$ $1.25 \pm 0.7$ $1.33 \pm 0.71$
LFW	Facenet	99.1	0.5	
CASIA	Facenet	99.5	0.6	
Celeb-A	ArcFace	64.1	7.0	$8.19 \pm 9.13$
LFW	ArcFace	50.8	1.4	$1.46 \pm 1.33$
CASIA	ArcFace	47.1	3.5	$1.57 \pm 2.81$

resolved simply by changing the scale factor. As mentioned in [23] as well, when we experimentally reduce the scale factor to improve security significantly, the TPR becomes unusably small. Thus, the poor trade-off between security and accuracy appears unavoidable for Facial-FE.

PIPE has over 89% ASR against Facial-FE, the prior scheme that claims to be a  $\ell_2$ -based fuzzy extractor.

PIPE **Against MRP.** Table 4 shows that PIPE succeeds with a high ASR of over 99.1% for Facenet models, and over 47.1% for ArcFace models. On the contrary, if we look at the partial leakage setting, PIPE performs poorly consistently with an ASR of less than 7%. This is in accordance with expectations since MRP maps embeddings to a smaller dimension randomly, and that randomness is not known in the case of partial leakage. Even though the Celeb-A arcface reconstruction accuracy is relatively higher, it is within 1 standard deviation of the mean of the random guessing success rate. Hence, PIPE reaffirms that though MRP provably satisfies the correctness Prop. 1 due to JL-Lemma, the privacy loss is severe in the full leakage setting.

All results reported in Table 4 are for output dimension n=128 for which target models retain good performance.

PIPE becomes even more effective for larger n and has an ASR of over 40% for  $n \geq 32$ . The input dimension is m = 512, the default for ArcFace and Facenet.

PIPE has ASR consistently above 47.1% against MRP under full leakage. It is significantly higher than the ASR under partial leakage, highlighting the security gap between full and partial leakage settings.

#### 6.3. Prior Attacks vs Partial Protection Schemes

We have shown that PIPE has high ASR against partial protection schemes. Are these partial protection schemes effective against prior attacks to begin with?

To answer this, we evaluate 3 state-of-the-art inversion attacks on face recognition models: Bob [14], KED-MI [30], GMI [31]. Bob is the state-of-the-art white-box embedding inversion attack which has reported better ASR than attacks preceding it. KED-MI and GMI are state-of-the-art black-box model inversion attacks<sup>6</sup> [17]. They both use GANs as the inversion model and have the best-known performance among black-box model inversion attacks [15].

**Evaluation Setup.** Note that KED-MI and GMI are technically designed to invert for closed-set face classification systems, i.e., to identify if an embedding corresponds to a particular member of a given set of faces. Closed-set classification differs from embedding inversion in that it requires training an additional classifier to map output embeddings to class labels corresponding to identities in the given closed set. To make these attacks workable for embedding inversion, we augment a classification layer on the target model, so that classifier outputs can be fed to these attacks as is. We use two disjoint subsets of the Celeb-A dataset corresponding to the same 1000 users to train and test the classification layer, and another disjoint subset of images to train the inversion model. The respective classifier accuracy is reported as well<sup>7</sup>.

There is a difference in how KED-MI and GMI attacks are evaluated. Since these 2 attacks are designed for a closed-set classification, they have to be tested on users whose identities have been seen during classifier training. The attack is considered successful if reconstructed images are classified by the target model to the correct identity class. On the other hand, PIPE and Bob are tested on unseen people (i.e. an open-set classification), which is more general and

<sup>6.</sup> The core of these attacks only requires black-box access to the target model, and a separate inversion model trained on the public dataset.

<sup>7.</sup> No classifier layer is used for PIPE and Bob and is reported as N/A.

TABLE 5: ASR (in %) of mentioned inversion attacks against unprotected Facenet and ArcFace embeddings. Inversion models are trained and evaluated on Celeb-A.

Attack	Model	ASR %	Classifier Acc %
PIPE	Facenet	<b>99.8</b>	N/A
Bob	Facenet	99.4	
KED-MI	Facenet	0.06	87.50
GMI	Facenet	0.02	
PIPE Bob	ArcFace ArcFace	<b>97.7</b> 96.4	N/A
KED-MI	ArcFace	0.16	90.96
GMI	ArcFace	0.08	

TABLE 6: ASR (in %) of mentioned inversion attacks against Facial FE-protected Facenet and ArcFace embeddings. Inversion models are trained and evaluated on Celeb-A.

Attack	Model	ASR %	Classifier Acc %
PIPE Bob	Facenet Facenet	<b>100.0</b> 95.4	N/A
KED-MI GMI	Facenet Facenet	0.02 0.02	73.9
PIPE Bob	ArcFace ArcFace	<b>95.8</b> 84.8	N/A
KED-MI GMI	ArcFace ArcFace	0.1 0.06	53.89

more challenging. So, PIPE and Bob are successful iff the  $\ell_2$  distance between the embeddings of the reconstructed images and corresponding original images is less than the threshold. Hence, the main comparison point to PIPE is Bob, which is also designed for (open-set) embedding inversion.

We evaluate both Facenet and ArcFace as target models under both unprotected and protected settings, using protection schemes: Facial-FE and MRP. Please see Appendix D for more details about the implementations of prior attacks.

Results. Tables 5 to 7 show that Bob is an effective inversion attack on unprotected embeddings, achieving an ASR exceeding 96.4% on both Facenet and ArcFace. Bob still achieves over 84.8% ASR with Facial-FE, underlining the weakness of Facial-FE in that a prior attack designed for unprotected embeddings alone is sufficient to recover private information. However, the performance of Bob falls drastically to 2.1% against MRP, suggesting that MRP works better than Facial-FE against Bob. In contrast, our adaptive PIPE attack remains effective for MRP and Facial-FE. It has ASR over 95% against Facial-FE and over 64% against MRP, indicating that PIPE is more powerful than Bob.

**Realistic images.** Figure 3 presents the representative images reconstructed by PIPE and Bob. Most PIPE reconstructions are accepted as the same face by the target model, which is *not* the case for Bob. Moreover, as seen in Tables 8 and 9, PIPE achieves a lower (better) visual similarity LPIPS score [9] and a lower (better) FID score [48]. This further

TABLE 7: ASR (in %) of mentioned inversion attacks against MRP-protected Facenet and ArcFace embeddings. Inversion models are trained and evaluated on Celeb-A.

Attack	Model	ASR %	Classifier Acc %
PIPE Bob	Facenet Facenet	<b>99.4</b> 0.2	N/A
KED-MI GMI	Facenet Facenet	0.10 0.04	71.34
PIPE Bob	ArcFace ArcFace	<b>64.1</b> 2.1	N/A
KED-MI GMI	ArcFace ArcFace	0.00 0.06	69.61



Figure 3: Reconstructed images by PIPE and Bob attacks against different protection schemes for Facenet embeddings. Check mark indicates successful authentication while cross indicates failure.

confirms that PIPE creates perceptually closer reconstructions to the original images (see Appendix E for details).

KED-MI and GMI attacks obtain less than 0.16% ASR on average over 5 trials, with or without a protection scheme. The weak performance of KED-MI and GMI is expected since these attacks rely solely on classification outputs, which are inherently more restrictive than using the embedding vector itself. We qualitatively inspected over 20 examples returned by these attacks, and we find that the reconstructions are quite far from the original consistently. Our implementation builds on code provided by [15].

PIPE attack is highly effective against prior partial defenses, with ASR ranging from 64% to over 99%. In contrast, the SOTA attack designed for embedding inversion, i.e. Bob attack, is mitigated by MRP, with ASR dropping from over 98% to below 0.1%.

## 7. Our Proposed Scheme: L2FE-Hash

We now propose a new  $\ell_2$ -based fuzzy extractor called L2FE-Hash that satisfies all requirements of an ideal primitive empirically. We formally characterize in Theorem 1 that L2FE-Hash has provable security when the benign distribution (of say faces) is well-behaved in a precise sense, regardless of what the adversary does. We further prove that FE realizes all 3 properties of ideal primitive in Theorem 2, even under full leakage. Hence L2FE-Hash can serve as

TABLE 8: LPIPS metric scores for Bob and PIPE attack

Durata ati an Calanna	Fac	enet	ArcFace	
<b>Protection Scheme</b>	Bob	PIPE	Bob	PIPE
Unprotected	0.28	0.21	0.20	0.20
Facial-FE	0.28	0.20	0.21	0.19
MRP	0.26	0.21	0.23	0.25
L2FE-Hash	0.49	0.27	0.38	0.27

TABLE 9: FID metric scores for Bob and PIPE attack

Ducto etian Calcana	Face	enet	ArcFace	
<b>Protection Scheme</b>	Bob	PIPE	Bob	PIPE
Unprotected	58.35	18.73	51.65	18.78
Facial-FE	58.67	17.93	52.51	17.03
MRP	69.56	20.87	69.87	20.20
L2FE-Hash	105.37	21.46	69.71	19.61

a secure ideal primitive construction when conditions of Theorem 1 are met. Our experiments in Section 8 confirm that L2FE-Hash defeats prior attacks we evaluated and PIPE.

**L2FE-Hash.** The L2FE-Hash scheme presented in Algo. 3 is a randomized lattice-based scheme that achieves  $\ell_2$  error correction and full-leakage security. Its GEN procedure constructs a random q-ary lattice from A and samples a random vector b, such that Ab gives us a random lattice point. It then computes a noisy version of the lattice point Ab + x where the input embedding x is treated as the noise. The ephemeral secret information b is hashed using a cryptographic hash function  $H_k$ . Only the public p, the hashed secret  $r = H_k(b)$ , and randomness (A, k) needed for authentication later are stored persistently in the database.

The REP procedure receives x'. It de-serializes p to obtain c=Ab+x that was computed during GEN. It implicitly checks if c-x' decodes to the correct ephemeral secret value by checking if the hash of the decoded value  $H_k(b)$  matches what is stored in the database. The Decode procedure is the well-known Babai's Nearest Plane (BNP) algorithm [49], which performs the  $\ell_2$  error correction.

## Algorithm 3 The L2FE-Hash construction.

```
1: procedure GEN
          Input: x \overset{\mathcal{X}}{\leftarrow} X

A \leftarrow \mathbb{Z}_q^{m \times l}, b \leftarrow \mathbb{Z}_q^l, k \leftarrow \{0, 1\}^{\lambda}

d := (A, Ab + x)
2:
                                                                                          \triangleright x \in \mathbb{Z}_q^m
3:
4:
5:
          p := (d, k) and r := H_k(b)
          return (r, p)
                                                           \triangleright r, p are stored persistently
6:
7: end procedure
    procedure REP
1:
2:
          Input: (x', p)
          Parse p as (A, c, k)

\beta := c - x'
3:
                                                                       \triangleright \beta is Ab + (x - x')
4:
                                                                           Decode is BNP
5:
          b := \operatorname{Decode}(A, \beta)
          return H_k(b)
7: end procedure
```

**L2FE-Hash is ideal.** L2FE-Hash can be considered a construction of the ideal primitive by renaming the secret r as y

and the helper p as s. The correctness of L2FE-Hash follows from the fact that during REP, we get a noisy lattice point  $\beta$  where the noise (x-x') has very small  $\ell_2$  norm when x,x' are close, i.e, are from the same user. Then BNP correction can successfully recover the lattice point Ab, which can be seen empirically in the reported accuracy of Section 8.

Intuitively, the security of L2FE-Hash stems from the following observation: An adversary who does not know an embedding x' close to the embedding x of the target user, cannot recover the secret b from the publicly leaked outputs (A, Ab + x) and  $H_k(b)$ . It is worth noting that without the hashing step, this scheme would no longer be secure under the full leakage scenario. Revealing bits of b would leak information about the input x. Therefore, hashing the secret is critical for achieving ideal security Prop. 2.

Formally Characterizing Security. Constructing a fuzzy extractor for an arbitrary family of distributions  $\mathcal X$  is known to be statistically impossible [50]. Therefore, to characterize the computational hardness of breaking L2FE-Hash, one must specialize to specific distributions. If we strictly confine the input face distribution  $\mathcal X$  to be discrete Gaussian or uniform over a small interval, then the hardness of recovering b from (A, Ab + x) is exactly the cryptographic hardness of the LWE problem [51], [52]. Nonetheless, this simplification is too unrealistic, as real-world face distributions are not known to follow any cryptographically hard distribution or have any closed-form mathematical characterization.

As the next best approach, we characterize the support of the distribution  $\mathcal X$  as a set of balls bounded in some  $[-R,R]^m$  space, since our application aims to correct within some  $\ell_2$  radius for a set of users. We refer to such distributions with high min-entropy h as well-behaved. Under the assumption that  $\mathcal X$  is uniform over the assumed support, we prove that L2FE-Hash is a secure FE where the number of secure output bits  $\kappa$  is upper bounded by some function of h. Theorem 1 makes the claim precise (see Appendix B for the proof). The L2FE-Hash output r is a  $\kappa$ -bitstring, but equivalently a vector in  $\mathbb Z_q^n$  as needed, where  $n=\kappa\log_q(2)$ .

**Theorem 1.** Let l, m, q, R > 0 be integers such that  $R \ge \alpha \sqrt{\frac{m}{2\pi e}} q^{1-l/m}$  for some  $\alpha > 1$ . Let  $C_{\epsilon} \subseteq [-R, R]^m$  be the union of  $\beta$  disjoint  $\epsilon$ -balls. Let  $\mathcal{X} = \mathcal{U}(C_{\epsilon})$  be uniform over  $C_{\epsilon}$ , with min entropy  $h = H_{\infty}(\mathcal{X})$ . Let Ext be an average case  $(l \log(q), \gamma, \kappa, \epsilon_{FE})$ -strong extractor given by universal hashing, where  $\gamma = h + m \log(\alpha) - m \log((2R+1))$ .

Then Algo. 3 satisfies the security property of an  $(C_{\epsilon}, \mathcal{X}, \kappa, t, \epsilon_{FE})$ -FE for any  $\kappa \leq \gamma - 2\log(1/\epsilon_{FE}) + 2$ , assuming that  $H_k$  in Algo. 3 is indistinguishable from Ext.

Remark 1. The above theorem offers a formal lens to understand when L2FE-Hash is provably secure. The distributional assumptions stated there are attack agnostic and do not constrain the attacker in any way—they merely characterize properties which, if the benign distribution  $\mathcal{X}$  satisfies, the provable security of L2FE-Hash will hold.

Remark 2. Theorem 1 assumes that input  $\mathcal{X}$  is uniform over  $C_{\epsilon}$ , but one could extend it to many useful well-behaved non-uniform distributions. Theorem 1 proves that

if  $\mathcal{X}$  is uniform over  $C_{\epsilon}$ , L2FE-Hash outputs are computationally indistinguishable from uniform, hence satisfying FE security. If  $\mathcal{X}$  is a non-uniform but well-behaved distribution with a bounded probability mass in each disjoint  $\epsilon$ -ball (user identity) of  $C_{\epsilon}$ , we conjecture that L2FE-Hash output will be a non-uniform distribution but still with sufficient minentropy. So, no poly-time adversary would be able to distinguish L2FE-Hash outputs from random given polynomially many samples, and the analogous security claim follows.

Choosing Practical Parameters. Theorem 1 specifies the minimum input entropy needed for good security for an abstract characterization of the distribution  $\mathcal{X}$ . But, determining entropy h for real distributions is intractable. So, we derive practical parameters such that the protected embeddings give good accuracy (TPR over 60%) and tractable runtime for GEN and REP. Note that once TPR exceeds well over 50%, majority voting over multiple independent face samples can boost it arbitrarily close to 100% [53]. To achieve accuracy of  $1-\delta$ , it suffices to have  $O(\log(1/\delta))$  face images of the user at authentication time, which can be run in parallel for efficiency. We evaluate L2FE-Hash using the best-known attacks, including prior ones and our PIPE attack on real datasets, to practically assess security.

Fuzzy Extractors and Ideal Defense. We have shown that L2FE-Hash is a provably secure fuzzy extractor for  $\ell_2$  distance if the input distribution  $\mathcal X$  satisfies certain conditions. Next, we state the desired connection between a fuzzy extractor and ideal defense primitive as Theorem 2. We defer the formal definition of these two primitives and the ideal primitive security game to Appendix A, and the proof of Theorem 2 to Appendix C due to space limits.

**Theorem 2.** Let FE be a  $(X, \mathcal{X}, \kappa, t, \epsilon_{FE})$ -fuzzy extractor as in [25]. Then FE is a  $(X, \mathcal{X}, \{0, 1\}^{\kappa}, t, \lambda)$ -ideal primitive with adversarial advantage  $Adv(\mathcal{A}) \leq \epsilon_{FE}(1 - \delta)$ .

# 8. Experimental Evaluation: L2FE-Hash

Following the same methodology and attack setup in Section 6, we now evaluate the security of L2FE-Hash experimentally against PIPE and other prior attacks we tested. We configure PIPE for L2FE-Hash as follows.

PIPE **Step 1 for L2FE-Hash.** For L2FE-Hash, similar to Facial-FE, we have public information p = (A, Ab + x, s) and private information  $r = H_s(b)$ . Since r is random, it cannot help the attack in any way. Hence in Step 1, we append the flattened matrix A to Ab + x, and use that as  $x^*$ .

**Practical L2FE-Hash Parameters.** All evaluations use embedding x projected to 180 dimensions for computational efficiency. The embedding is quantized<sup>8</sup> to  $\mathbb{Z}_q$ , and then scaled down by a scale hyperparameter optimized for BNP correction. The hyperparameters used for L2FE-Hash protection scheme are m=180, l=60, q=130003 with

8. For embedding x, the quantized embedding is  $\lfloor (x-\min)/(\max-\min) * q* \text{scale} \rfloor$  where  $\min$  and  $\max$  are the smallest and largest elements of any embedding vector in the Celeb-A train dataset.

TABLE 10: Cross-Dataset ASR (in %) of PIPE attack against L2FE-Hash-protected embeddings and Success Probability of Random Guessing (± standard deviation). Training set is Celeb-A.

Test set	Model	PIPE %	Random %
Celeb-A	Facenet	0.6	$1.01 \pm 0.52$
LFW	Facenet	0.5	$1.25 \pm 0.7$
CASIA	Facenet	0.4	$1.33 \pm 0.71$
Celeb-A	ArcFace	7.0	$8.19 \pm 9.13$
LFW	ArcFace	1.7	$1.46 \pm 1.33$
CASIA	ArcFace	3.3	$1.57 \pm 2.81$

TABLE 11: ASR (in %) of mentioned inversion attacks against L2FE-Hash-protected Facenet and ArcFace embeddings. Inversion models are trained and evaluated on Celeb-A dataset.

Attack	Model	ASR %	Classifier Acc %
PIPE	Facenet	0.60	N/A
Bob	Facenet	0.60	
KED-MI	Facenet	0.06	50.33
GMI	Facenet	0.04	
PIPE	ArcFace	7.0	N/A
Bob	ArcFace	7.0	
KED-MI	ArcFace	0.1	38.33
GMI	ArcFace	0.08	

scale = 0.0014, 0.0017 for Facenet and ArcFace respectively. These remain the same throughout our evaluation.

PIPE **Against L2FE-Hash.** Table 10 reports the ASR of PIPE against L2FE-Hash to be at most 7% for all datasets. This is within one standard deviation of the mean ASR for random guessing, which is expected for a secure scheme.

**Prior Attacks against L2FE-Hash.** Table 11 shows that all 4 attacks—PIPE, Bob, GMI and KED-MI—have poor ASR against L2FE-Hash, unlike for partial protection schemes. The ASR is below 0.6% for Facenet embeddings and below 7% for ArcFace embeddings, and always within one standard deviation of the average ASR of random guessing.

All evaluated attacks, including PIPE, fail consistently against L2FE-Hash, highlighting its practical security.

Accuracy of Face Recognition with L2FE-Hash. To be practically usable, L2FE-Hash must have reasonably good accuracy, while defending against model inversion. We evaluate L2FE-Hash for 100 pairs of same user images and 100 pairs of different user images from Celeb-A dataset. From Table 12, we observe that L2FE-Hash has above 60% TPR for both target models (feature extractors) with FPR less than 26%. Since the TPR  $\geq 50\%$  and FPR  $\leq 50\%$ , one can employ majority voting over multiple independent samples of the user's face to boost the accuracy overall as needed, as previously mentioned in Section 7 [53].

TABLE 12: BNP correction results (in %) against L2FE-Hash embeddings on Celeb-A dataset. The number in  $(\cdot)$  indicates the scale by which embeddings are compressed in the  $\mathbb{Z}_q$  space.

Actual \ Predicted	ual \ Predicted   Facenet (0.0014)   ArcFace (0.0014)   Positive   Positive			
Positive	65	35	60	40
Negative	4	96	26	74

## 9. Related Work

An embedding inversion attack is a canonical example of model inversion attacks that targets model embeddings [7]. A number of model inversion attacks on image recognition ML models have been developed, often targeting image classification outputs [29], [30], [31], [54], [55]. There are also model inversion attacks on face authentication systems that target image embeddings [13], [14]. We have evaluated 3 prior attacks representative of SOTA attack accuracy.

Gradient inversion attacks [56] require more than just model outputs and do not meet the original definitions of model inversion [7]. They are not in scope of our defenses.

Non-post-processing defenses. Many defenses against model inversion modify the training process, not post-processing outputs of ML models already trained [15], [16], [17], [18]. Being highly model-specific and optimization-based, it is hard to theoretically characterize their end security guarantees. Their recently reported effectiveness against existing black-box attacks is fairly limited, with attacks re-identifying  $\geq 30\%$  of users from reconstructed images from models that have accuracy over  $\geq 80\%$  [15], [17]. Importantly, our work points towards defining properties of cryptographic defenses that generically work with ML models for authentication and in an attack-agnostic way.

The privacy risk from model inversion is immediate, which is our primary concern. There is also re-authentication risk, i.e., using recovered face images to impersonate the user. Liveness detectors during face authentication mitigate such risks, but a line of prior works originating with Xu et. al. [57] shows attacks against such mechanisms. These techniques are complementary to mechanisms we study.

Post-processing protection schemes. Most post-processing protection mechanisms for embedding vectors are some variant of MRP, or use other non-invertible transformations that do not satisfy fuzzy one-wayness (Prop. 2). For example, BioHashing is MRP followed by a binary quantization step, and it is known to have pre-image attacks [34], [58], [59]. Index-of-Max Hashing performs random projection on fingerprint minutiae and is also vulnerable [35], [60]. In fact, many protection mechanisms that rely on a distance-preserving transformation are vulnerable to pre-image attacks [61], [62], and thus do not satisfy Prop. 2. There are also schemes that combine MRP with fuzzy commitment for additional security, but they still do not address inversion attacks that recover approximately close inputs [63], [64].

Similarly, fuzzy hashes, or locality-sensitive hashes [65], [66] aim to find linear projections that preserve local in-

formation. For example, Apple's NeuralHash trains a CNN model to learn such mappings for security applications, but it remains vulnerable to adversarial attacks that force hash collisions [3], [67]. Furthermore, CNN models in general are particularly susceptible to model inversion attacks [39].

Other fuzzy extractor schemes have been proposed, such as the LWE-FE [68]. While being similar to our L2FE-Hash, it has a different decoder construction that targets the  $(\ell_0$  norm) Hamming distance. Moreover, it assumes the input distribution to be uniform over a small interval or LWE-admissible, which is an extremely strong assumption for real face distributions. To our knowledge, no prior work gives a secure FE construction for  $\ell_2$  distances under assumptions that even approximately models real-world distributions and yet shows reasonable accuracy in practical setups.

Other Threat Models. Our L2FE-Hash security definition under full-leakage threat model is not to be confused with post-compromise security. The latter addresses the issue of secure encryption of future messages after key leakage, whereas Prop. 2 addresses the issue of information leakage about past messages after key leakage [69].

Prop. 2 is also different from forward secrecy, a property of key-exchange protocols ensuring that compromising a long-term key does not reveal past session keys [70]. The fundamental idea that a compromise should not lead to decrypting past messages is similar to L2FE-Hash, but our setting is different from a key-exchange protocol. We additionally assume past encrypted messages, which in our context are protected embeddings, can be compromised.

Honey encryption (HE) addresses a different threat model from ours [71]. It allows for encryption of passwords with low entropy keys such that decryption with incorrect keys yields honey messages—messages that occur as likely as the original message but are hard to guess without a database breach [71], [72]. We consider the event of full database breach. HE makes it difficult for the adversary to distinguish correct from incorrect decryption, thwarting offline message recovery attacks. It can aid in breach detection by alerting when an adversary unknowingly queries the database with the honeyword. Moreover, password encryption schemes generally do not require locality-sensitivity.

#### 10. Conclusions

We have shown that fuzzy extractors offer an attack-agnostic and model-agnostic defense against model inversion attacks on embeddings leaked from a database breach. Our PIPE attack demonstrates that prior partially-secure primitives are insecure in this context. We have proposed L2FE-Hash, a fuzzy extractor for vector inputs that enables comparators in Euclidean norm, offering strong security even when all persistently stored data is leaked in the breach.

# 11. Ethical Considerations

All the datasets used in this paper, Casia-Webface [43], Celeb-A [45] and LFW [47], have licenses which allow their

use for face verification tasks for research purposes. We do not foresee ethical issues arising from our work, as we have shown both powerful attacks and a strong defense.

## References

- [1] J. Deng, J. Guo, N. Xue, and S. Zafeiriou, "Arcface: Additive angular margin loss for deep face recognition," in *IEEE/CVF Conf. Comput. Vis. Pattern Recognit. (CVPR)*, 2019.
- [2] F. Schroff, D. Kalenichenko, and J. Philbin, "Facenet: A unified embedding for face recognition and clustering," in *IEEE Conf. Comput. Vis. Pattern Recognit. (CVPR)*, 2015.
- [3] Apple Incorporated. (2021) Csam detection. https://www.apple. com/child-safety/pdf/CSAM\_Detection\_Technical\_Summary.pdf. Accessed: 12 November 2024.
- [4] T. Liu. (2023) How we store and search 30 billion faces. https://www.clearview.ai/post/how-we-store-and-search-30-billion-faces. Clearview AI. Accessed: Oct. 23, 2025.
- T. de Lachèze-Murel. (2023) Biometric-enabled wallets. https://www. dfns.co/article/biometric-enabled-wallets. Dfns. Accessed: 23 October 2025.
- [6] "Outabox data breach exposes 1m biometric records," https://www.aiaaic.org/aiaaic-repository/ai-algorithmic-and-automation-incidents/outabox-data-breach-exposes-1m-biometric-records, AIAAIC, 2024, accessed April 7, 2025.
- [7] M. Fredrikson, S. Jha, and T. Ristenpart, "Model inversion attacks that exploit confidence information and basic countermeasures," in Proc. 22nd ACM SIGSAC Conf. Comput. Commun. Sec., 2015.
- [8] S. Minaee, N. Kalchbrenner, E. Cambria, N. Nikzad, M. Chenaghlu, and J. Gao, "Deep learning based text classification: A comprehensive review," ACM Comput. Surveys (CSUR), 2021.
- [9] R. Zhang, P. Isola, A. A. Efros, E. Shechtman, and O. Wang, "The unreasonable effectiveness of deep features as a perceptual metric," in *Proc. IEEE Conf. Comput. Vis. Pattern Recognit. (CVPR)*, 2018.
- [10] Y. Gao, Y. Xiong, X. Gao, K. Jia, J. Pan, Y. Bi, Y. Dai, J. Sun, H. Wang, and H. Wang, "Retrieval-augmented generation for large language models: A survey," arXiv:2312.10997, 2024.
- [11] A. Ramesh, M. Pavlov, G. Goh, S. Gray, C. Voss, A. Radford, M. Chen, and I. Sutskever, "Zero-shot text-to-image generation," in Int. Conf. Mach. Learn., 2021.
- [12] H. Otroshi Shahreza and S. Marcel, "Face reconstruction from facial templates by learning latent space of a generator network," in Adv. Neural Inf. Process. Syst., 2023.
- [13] M. Kansy, A. Raël, G. Mignone, J. Naruniec, C. Schroers, M. Gross, and R. M. Weber, "Controllable inversion of black-box face recognition models via diffusion," in *IEEE/CVF Int. Conf. Comput. Vis. Workshops (ICCVW)*, 2023.
- [14] H. O. Shahreza, V. K. Hahn, and S. Marcel, "Vulnerability of state-of-the-art face recognition models to template inversion attack," *IEEE Trans. Inf. Forensics Sec.*, 2024.
- [15] X. Peng, F. Liu, J. Zhang, L. Lan, J. Ye, T. Liu, and B. Han, "Bilateral dependency optimization: Defending against model-inversion attacks," in *Proc. 28th ACM SIGKDD Conf. Knowl. Discov. Data Min.*, 2022.
- [16] T. Wang, Y. Zhang, and R. Jia, "Improving robustness to model inversion attacks via mutual information regularization," in *Proc.* AAAI Conf. Artif. Intell., 2021.
- [17] V.-H. Tran, N.-B. Nguyen, S. T. Mai, H. Vandierendonck, and N.-m. Cheung, "Defending against model inversion attacks via random erasing," arXiv:2409.01062, 2024.
- [18] X. Gong, Z. Wang, S. Li, Y. Chen, and Q. Wang, "A gan-based defense framework against model inversion attacks," *IEEE Trans. Inf. Forensics Sec.*, 2023.

- [19] B. Pal, T. Daniel, R. Chatterjee, and T. Ristenpart, "Beyond credential stuffing: Password similarity models using neural networks," in *IEEE Symp. Sec. Privacy (SP)*, 2019.
- [20] R. Morris and K. Thompson, "Password security: a case history," Commun. ACM, 1979.
- [21] C. Rathgeb and A. Uhl, "A survey on biometric cryptosystems and cancelable biometrics," EURASIP J. Inf. Sec., 2011.
- [22] B. Choudhury, P. Then, B. Issac, V. Raman, and M. K. Haldar, "A survey on biometrics and cancelable biometrics systems," *Int. J. Image Graph.*, 2018.
- [23] K. Zhang, H. Cui, and Y. Yu, "Facial template protection via lattice-based fuzzy extractors," *Cryptology ePrint Archive*, 2021.
- [24] A. B. J. Teoh and C. T. Yuang, "Cancelable biometrics realization with multispace random projections," *IEEE Trans. Syst., Man, and Cybern.*, Part B (Cybern.), 2007.
- [25] Y. Dodis, L. Reyzin, and A. Smith, "Fuzzy extractors: How to generate strong keys from biometrics and other noisy data," in Adv. Cryptology - EUROCRYPT, 2004.
- [26] D. Bratić, F. Vešović, and V. Mijanović, "Audio watermarking under gradient-based reconstruction attack," in 5th Mediterr. Conf. Embed. Comput. (MECO), 2016.
- [27] R. Zhang, S. Hidano, and F. Koushanfar, "Text revealer: Private text reconstruction via model inversion attacks against transformers," arXiv:2209.10505, 2022.
- [28] V. Costan and S. Devadas, "Intel SGX explained," Cryptology ePrint Archive, 2016.
- [29] N.-B. Nguyen, K. Chandrasegaran, M. Abdollahzadeh, and N.-M. Cheung, "Re-thinking model inversion attacks against deep neural networks," in *Proc. IEEE/CVF Conf. Comput. Vis. Pattern Recognit.* (CVPR), 2023.
- [30] S. Chen, M. Kahla, R. Jia, and G.-J. Qi, "Knowledge-enriched distributional model inversion attacks," in *Proc. IEEE/CVF Int. Conf. Comput. Vis.*, 2021.
- [31] Y. Zhang, R. Jia, H. Pei, W. Wang, B. Li, and D. Song, "The secret revealer: Generative model-inversion attacks against deep neural networks," in *Proc. IEEE/CVF Conf. Comput. Vis. Pattern Recognit.* (CVPR), 2020.
- [32] A. Kanta, I. Coisel, and M. Scanlon, "A survey exploring open source intelligence for smarter password cracking," *Forensic Sci. Int.: Digital Investig.*, 2020.
- [33] N. Li, F. Guo, Y. Mu, W. Susilo, and S. Nepal, "Fuzzy extractors for biometric identification," in *IEEE 37th Int. Conf. Distrib. Comput.* Syst. (ICDCS), 2017.
- [34] A. T. B. Jin, D. N. C. Ling, and A. Goh, "Biohashing: two factor authentication featuring fingerprint data and tokenised random number," *Pattern Recognit.*, 2004.
- [35] Z. Jin, J. Y. Hwang, Y.-L. Lai, S. Kim, and A. B. J. Teoh, "Ranking-based locality sensitive hashing-enabled cancelable biometrics: Index-of-Max Hashing," *IEEE Trans. Inf. Forensics Sec.*, 2017.
- [36] W. Johnson and J. Lindenstrauss, "Extensions of lipschitz maps into a hilbert space," *Contemp. Math*, 1984.
- [37] S. Dasgupta and A. Gupta, "An elementary proof of a theorem of Johnson and Lindenstrauss," *Random Struct. Algorithms*, 2003.
- [38] R. Penrose, "A generalized inverse for matrices," *Math. Proc. Camb. Philos. Soc.*, 1955.
- [39] H. O. Shahreza, V. K. Hahn, and S. Marcel, "Face reconstruction from deep facial embeddings using a convolutional neural network," in *IEEE Int. Conf. Image Process. (ICIP)*, 2022.
- [40] P. Dhariwal and A. Nichol, "Diffusion models beat GANs on image synthesis," Adv. Neural Inf. Process. Syst., 2021.

- [41] S. Serengil and A. Özpınar, "A benchmark of facial recognition pipelines and co-usability performances of modules," *Bilişim Teknolojileri Dergisi*, 2024.
- [42] Q. Cao, L. Shen, W. Xie, O. M. Parkhi, and A. Zisserman, "Vg-gface2: A dataset for recognising faces across pose and age," arXiv:1710.08092v2, 2018.
- [43] D. Yi, Z. Lei, S. Liao, and S. Z. Li, "Learning face representation from scratch," arXiv:1411.7923, 2014.
- [44] J. Xiang and G. Zhu, "Joint face detection and facial expression recognition with MTCNN," in 4th Int. Conf. Inf. Sci. Control Eng. (ICISCE), 2017.
- [45] Z. Liu, P. Luo, X. Wang, and X. Tang, "Deep learning face attributes in the wild," in *Proc. of Int. Conf. Comput. Vis. (ICCV)*, 2015.
- [46] S. I. Serengil, "Chefboost: A lightweight boosted decision tree framework," https://doi.org/10.5281/zenodo.5576203, 2021.
- [47] G. B. Huang, M. Mattar, H. Lee, and E. Learned-Miller, "Learning to align from scratch," in NIPS, 2012.
- [48] M. Heusel, H. Ramsauer, T. Unterthiner, B. Nessler, and S. Hochreiter, "Gans trained by a two time-scale update rule converge to a local nash equilibrium," in *Proc. 31st Int. Conf. Neural Inf. Process. Syst.* (NIPS), 2017.
- [49] L. Babai, "On lovász' lattice reduction and the nearest lattice point problem," Combinatorica, 1986.
- [50] B. Fuller, L. Reyzin, and A. Smith, "When are fuzzy extractors possible?" *IEEE Trans. Inf. Theory*, 2020.
- [51] O. Regev, "On lattices, learning with errors, random linear codes, and cryptography," in *Proc. 37th Annu. ACM Symp. Theory Comput.* (STOC), 2005.
- [52] N. Döttling and J. Müller-Quade, "Lossy codes and a new variant of the learning-with-errors problem," in Adv. Cryptology – EURO-CRYPT, 2013
- [53] A. R. Webb and K. D. Copsey, Statistical Pattern Recognition, 2011.
- [54] K.-C. Wang, Y. FU, K. Li, A. Khisti, R. Zemel, and A. Makhzani, "Variational model inversion attacks," in Adv. Neural Inf. Process. Syst., 2021.
- [55] X. Yuan, K. Chen, J. Zhang, W. Zhang, N. Yu, and Y. Zhang, "Pseudo label-guided model inversion attack via conditional generative adversarial network," in *Proc. 37th AAAI Conf. Artif. Intell. (AAAI)*, 2023.
- [56] L. Zhu, Z. Liu, and S. Han, "Deep leakage from gradients," Adv. Neural Inf. Process. Syst., 2019.
- [57] Y. Xu, T. Price, J.-M. Frahm, and F. Monrose, "Virtual U: Defeating face liveness detection by building virtual models from your public photos," in 25th USENIX Sec. Symp. (USENIX), 2016.
- [58] K. H. Cheung, A. W.-K. Kong, J. You, D. Zhang et al., "An analysis on invertibility of cancelable biometrics based on biohashing." in CISST, 2005.
- [59] Y. Lee, Y. Chung, and K. Moon, "Inverse operation and preimage attack on biohashing," in *IEEE Workshop Comput. Intell. in Biometrics: Theory, Algorithms, Appl.*, 2009.
- [60] L. Ghammam, K. Karabina, P. Lacharme, and K. Thiry-Atighehchi, "A cryptanalysis of two cancelable biometric schemes based on indexof-max hashing," *IEEE Trans. Inf. Forensics Sec.*, 2020.
- [61] X. Dong, J. Park, Z. Jin, A. B. J. Teoh, M. Tistarelli, and K. Wong, "On the security risk of pre-image attack on cancelable biometrics," J. King Saud Univ. Comput. Inf. Sci., 2024.
- [62] X. Dong, Z. Jin, and A. T. B. Jin, "A genetic algorithm enabled similarity-based attack on cancellable biometrics," in *IEEE 10th Int.* Conf. Biometrics Theory, Appl. Syst. (BTAS), 2019.
- [63] T. A. T. Nguyen, T. K. Dang, and D. T. Nguyen, "A new biometric template protection using random orthonormal projection and fuzzy commitment," arXiv:1904.00264, 2019.

- [64] T. A. Thao Nguyen, T. K. Dang, and D. T. Nguyen, "Non-invertibility for random projection based biometric template protection scheme," in 15th Int. Conf. Ubiquitous Inf. Manag. and Commun. (IMCOM), 2021.
- [65] A. Gionis, P. Indyk, R. Motwani et al., "Similarity search in high dimensions via hashing," in Vldb, 1999.
- [66] K. Zhao, H. Lu, and J. Mei, "Locality preserving hashing," in Proc. AAAI Conf. Artif. Intell., 2014.
- [67] L. Struppek, D. Hintersdorf, D. Neider, and K. Kersting, "Learning to break deep perceptual hashing: The use case neuralhash," in ACM Conf. Fairness, Accountability, and Transparency (FAccT), 2022.
- [68] B. Fuller, X. Meng, and L. Reyzin, "Computational fuzzy extractors," Inf. Comput., 2020.
- [69] K. Cohn-Gordon, C. Cremers, and L. Garratt, "On post-compromise security," in *IEEE 29th Comput. Sec. Foundations Symp. (CSF)*, 2016.
- [70] H. Krawczyk, Perfect Forward Secrecy, 2019.
- [71] A. Juels and T. Ristenpart, "Honey encryption: Security beyond the brute-force bound," in Adv. Cryptology – EUROCRYPT, 2014.
- [72] K. C. Wang and M. K. Reiter, "Bernoulli honeywords," in Proc. 2024 Netw. Distrib. Syst. Sec. Symp. (NDSS), 2024.
- [73] J. Håstad, R. Impagliazzo, L. A. Levin, and M. Luby, "A pseudorandom generator from any one-way function," SIAM J. Comput., 1999.
- [74] J. W. S. Cassels, An introduction to the geometry of numbers, 1996.
- [75] T. Esler, "Face recognition using pytorch," https://github.com/ timesler/facenet-pytorch, 2019.
- [76] M. Seitzer, "pytorch-fid: FID Score for PyTorch," https://github.com/ mseitzer/pytorch-fid, 2020, version 0.3.0.
- [77] O. M. Parkhi, A. Vedaldi, and A. Zisserman, "Deep face recognition," in *British Machine Vision Conf.*, 2015.

# Appendix A. Formalization of the Ideal Primitive

We present the formal definition of the idealized primitive introduced in Section 3, with the formal security game.

**Notation.** Aside from symbols specified in Table 1, we use uppercase alphabets for sets, metric spaces, and random variables. We use uppercase cursive alphabets for probability distributions. Specifically,  $\mathcal{U}(S)$  denotes the uniform random distribution over the set S. We use  $\overset{\mathcal{D}}{\leftarrow} Q$  to denote sampling from a set Q according to distribution  $\mathcal{D}$ , or simply  $\leftarrow \mathcal{D}$  when the underlying set is obvious from context. X and Y are input and output sets from a metric space with  $d = \ell_2$  distance, such as  $X = \mathbb{R}^m$  and  $Y = \mathbb{R}^n$ . The ball  $B_m(x,t)$  is the set of all vectors within distance t of  $x \in \mathbb{R}^m$ . We also use B(x,t) or  $B_m(t)$  to denote the ball  $B_m(x,t)$  when the omitted variable is clear from context.

#### A.1. Formal definition

**Definition 3** (Ideal primitive). A  $(X, X, Y, t, \lambda)$  ideal primitive is a pair of randomized procedures, "generate" (GEN) and "reproduce" (REP). GEN on input  $x \in X$  outputs a seed  $s \in \{0,1\}^{\lambda}$  and  $y \in Y$ . REP takes  $x' \in X$  and  $s \in \{0,1\}^{\lambda}$  as inputs and gives some  $y' \in Y$  as output. (GEN, REP) have the following properties:

1) Correctness (Noise tolerance): If  $d(x, x') \le t$  and (s, y) = GEN(x), then

$$\Pr[y = \operatorname{Rep}(x', s))] \ge 1 - \delta.$$

- 2) Security (Fuzzy one-way): Given (s,y) from Gen(x) where  $x \overset{\mathcal{X}}{\leftarrow} X$ , it is hard to find x' such that  $d(x,x') \leq t$ . In other words, for any computationally bounded adversary  $\mathcal{A}$  trying to find such x', its advantage is negligible, i.e.  $Adv(\mathcal{A}) \leq negl(\lambda)$  (see Eqn (2) for definition of Adv).
- 3) Utility (Entropy sufficiency): Let  $\mathcal{Y}$  and  $\mathcal{S}$  be the output distributions of GEN for an input distribution  $\mathcal{X}$ . The HILL entropy of  $\mathcal{Y}|\mathcal{S}$  is at least the min entropy of  $\mathcal{X}$ .

The probability in Prop. 1 is taken over  $x' \overset{\mathcal{X}}{\leftarrow} B(x,t)$  and  $x \overset{\mathcal{X}}{\leftarrow} X$ . The  $\delta$  term in Prop. 1 can be any value in [0,1]. It only affects functional correctness, such as the false positives and negatives in the authentication application. On the other hand, "hardness" in Prop. 2 is cryptographic, i.e., the probability of an adversary violating Prop. 2 should be a negligible function in  $\lambda$ . We consider a computationally bounded adversary that runs in  $\operatorname{poly}(\lambda)$  time. We formalize the security game of Prop. 2 in Section A.2. In Prop. 3, HILL entropy is the computational notion of min entropy [73].

## A.2. Formal Security game

To make Prop. 2 precise, we define two notions of indistinguishability below. We use the computational version for Prop. 2 and the security game is given below.

**Definition 4** (Statistical indistinguishability). Let X and Y be random variables with supports  $S_X$  and  $S_Y$  respectively. The statistical distance between X and Y is defined as

$$SD(X,Y) := \frac{1}{2} \sum_{u \in S_X \cup S_Y} |\Pr[X = u] - \Pr[Y = u]|$$

If  $SD(X,Y) \leq \epsilon$ , we denote  $X \stackrel{stat}{\approx} Y$ . If  $\epsilon$  is negligibly small, we say X and Y are statistically indistinguishable.

**Definition 5** (Computational indistinguishability). Let X and Y be random variables. For a probabilistic polynomialtime (PPT) algorithm A and a security parameter  $\lambda$ , the adversarial advantage of distinguishing them is defined as

$$Adv(\mathcal{A}) = |\Pr[\mathcal{A}(X) = 1] - \Pr[\mathcal{A}(Y) = 1]|$$

If  $Adv(A) \leq \epsilon$  for all PPT A, denote  $X \stackrel{comp}{\approx} Y$ . If  $\epsilon$  is negligible in  $\lambda$ , X and Y are **computationally indistinguishable**.

**Security Game.** Let the input distribution  $\mathcal{X}$  over X be public information. The game G consists of adversary  $\mathcal{A}$  and challenger  $\mathcal{C}$  doing the following:

- 1) Challenger C samples  $x \overset{\mathcal{X}}{\leftarrow} X$ , computes (s,y) = GEN(x), and gives (s,y) to adversary A.
- 2) A receives (s, y) and outputs x'.
- 3)  $\mathcal{A}$  wins if  $x' \in B(x,t)$ . G returns 1 if  $\mathcal{A}$  wins, else 0.

The advantage of the adversary A is defined as:

$$Adv(\mathcal{A}) = \Pr[G(\mathcal{A}, \mathcal{C}) = 1] - \Pr[G(\mathcal{A}', \mathcal{C}) = 1]$$
 (2)

where  $\mathcal{A}'$  is the best baseline adversary that only utilizes s and  $\mathcal{X}$  but not y at step 2. If  $Adv(\mathcal{A})$  is negligible for all adversaries  $\mathcal{A}$ , then Prop. 2 is satisfied.

# Appendix B. Theoretical Security of L2FE-Hash

We prove that L2FE-Hash satisfies FE security under the assumption that the input distribution is uniform over a bounded support consisting of multiple disjoint  $\epsilon$ -radius balls, as in Theorem 1. The center of each  $\epsilon$ -ball can be seen as the representative embedding of a user. Then the  $\epsilon$ -ball around the center represents the cluster of embeddings corresponding to that user. L2FE-Hash is a FE.

#### **B.1.** Definitions

A fuzzy extractor (FE) extracts a uniformly random string with error tolerance. It was first proposed by [25], and [50] relaxed the definition to account for  $\delta$  error in correctness. We adapt the definition of FE with  $\delta$  errors by [50] for a specific input distribution in Definition 6. Let M be a metric space with distance metric d, and  $\mathcal X$  be a distribution over M.

**Definition 6** (Fuzzy Extractor with Error). An  $(M, \mathcal{X}, \kappa, t, \epsilon_{FE})$ -fuzzy extractor with error  $\delta$  is a pair of randomized procedures, "generate" (GEN) and "reproduce" (REP). GEN on input  $w \in M$  outputs an extracted string  $r \in \{0,1\}^{\kappa}$  and a helper string  $p \in \{0,1\}^{\kappa}$ . REP takes  $w' \in M$  and  $p \in \{0,1\}^{\kappa}$  as inputs, and outputs  $r' \in \{0,1\}^{\kappa}$ . (GEN, REP) have the following properties:

- 1) Correctness: If  $d(w,w') \leq t$  and (r,p) = Gen(w), then  $\Pr[\text{Rep}(w',p)=r] \geq 1-\delta$ . If d(w,w') > t, then no guarantee is provided about the output of Rep.
- 2) Security: For input distribution  $\mathcal{X}$ , if  $(\mathcal{R}, \mathcal{P}) = Gen(\mathcal{X})$ , then  $(\mathcal{R}, \mathcal{P}) \approx_{\epsilon_{FE}} (\mathcal{U}(\{0,1\}^{\kappa}), \mathcal{P})$ .

The security property of Definition 6 requires the string r to be nearly uniform even for those who observe p. The notation  $\approx_{\epsilon_{\rm FE}}$  represents both notions of indistinguishability as defined in Section A.2.

The strong extractor primitive (Definition 7) is commonly used to construct fuzzy extractors. It can be implemented as a universal hash function, and can extract  $\kappa \leq \gamma - 2\log(1/\epsilon_{\rm FE}) + 2$  many bits of randomness, effectively transforming a high entropy input (Definition 11) into a uniformly distributed output (see Lemma 2.4 in [25]).

**Definition 7** (Strong extractor [25, Section 2.5]). Let  $Ext: \{0,1\}^l \to \{0,1\}^\kappa$  be a polynomial time probabilistic function using  $\lambda$  bits of randomness. Ext is an efficient average-case  $(l,\gamma,\kappa,\epsilon_{FE})$ -strong extractor if for all pairs of random variables (X,I) such that X is an l-bit string satisfying  $\tilde{H}_{\infty}(X|I) \geq \gamma$ , we have  $SD((Ext(X;K),K,I),(\mathcal{U}(\{0,1\}^\kappa),K,I)) \leq \epsilon_{FE}$ , where K is uniform on  $\{0,1\}^\lambda$ .

Now we present the definition of several terms used to characterize the input distribution and used in the proof.

**Definition 8** (R-bounded). For an integer R > 0, an mdimensional set X is R-bounded if in each dimension, its values are bounded between [-R, R], i.e.  $X \subseteq [-R, R]^m$ .

**Definition 9**  $(C_{\epsilon})$ . For  $\epsilon > 0$  and some integer R > 0, let  $C \subset [-R+\epsilon, R-\epsilon]^m$  be a closed set of size  $\beta$  such that  $\forall c_1, c_2 \in C$  where  $c_1 \neq c_2$ ,  $||c_1 - c_2||_2 > 2\epsilon$ . Then  $C_{\epsilon}$ denotes the union of disjoint  $\epsilon$ -balls with centers in C, i.e.

$$C_{\epsilon} = \{p \colon ||p - p'||_2 \le \epsilon \text{ for some } p' \in C\} \subset [-R, R]^m.$$

**Definition 10** (Ambiguity). We say that a vector  $\mathbf{y} \in \mathbb{Z}_q^m$ is N-ambiguous for a matrix A and an error distribution  $\mathcal{X}$ , if  $|\{\mathbf{b} \in \mathbb{Z}_q^l \mid \mathbf{y} - \mathbf{A}\mathbf{b} \in supp(\mathcal{X})\}| \geq N$ . If A and  $\mathcal{X}$ are clear by context, we just say that y is N-ambiguous.

**Definition 11** (Min Entropy [25, Section 2.4]). Let log denote the base 2 logarithm. Let (X,Y) be a pair of random variables. Define min entropy of X as  $H_{\infty}(X) =$  $-\log(\max_x \Pr[X = x])$ , and the average (conditional) **min-entropy** of X given Y as

$$\tilde{H}_{\infty}(X|Y) = -\log\left(\mathbb{E}_{y \leftarrow Y} \max_{x} \Pr[X = x|Y = y]\right).$$

## **B.2. Proof of Intermediate Theorem**

Before proving Theorem 1, we first prove that the public information d = (A, Ab + x) of L2FE-Hash in Algo. 3 has high entropy, as stated in Theorem 12.

**Theorem 12.** Let l, m, q, R > 0 be integers such that  $R \ge$  $\alpha\sqrt{\frac{m}{2\pi e}}q^{1-l/m}$  for some  $\alpha>1$ . Let  $\mathcal{X}=\mathcal{U}(C_{\epsilon})$  and h=0 $H_{\infty}(\mathcal{X})$ . Let **A** be distributed according to  $\mathcal{U}(\mathbb{Z}_q^{m \times l})$ . Let  $\mathbf{y} = \mathbf{A}\mathbf{b}' + \mathbf{x}'$ , with  $\mathbf{b}' \leftarrow \mathcal{U}(\mathbb{Z}_q^l)$  and  $\mathbf{x}' \leftarrow \mathcal{X}$ . Also let  $\mathbf{b} \leftarrow \mathcal{U}(\mathbb{Z}_q^l)$  and  $\mathbf{x} \leftarrow \mathcal{X}$ , then with probability  $1 - 1/q^{m-l}$ ,

$$\tilde{H}_{\infty}(\mathbf{b}|\mathbf{Ab}+\mathbf{x}=\mathbf{y}) \geq \gamma(h)$$

where  $\gamma(h) = h + m \log(\alpha) - m \log((2R+1))$ .

**Proof of Theorem 12.** Define p to be the probability that an integer point chosen uniformly at random from  $[-R, R]^m$ lands in  $C_{\epsilon}$ . We get **Fact 1**: that  $p:=\frac{f(\beta,\epsilon,m)}{(2R+1)^m}=\frac{2^h}{(2R+1)^m}$  since by Lemma 3, we know that  $f(\beta,\epsilon,m)=2^h$ .

Consider a random matrix  $\mathbf{A} \in \mathbb{Z}_q^{m \times l}$ . The corresponding q-ary lattice is  $\mathcal{L}(\mathbf{A}) = \{x \mid x = \mathbf{A}s\}$ 

responding q-ary fattice is 
$$\mathcal{L}(\mathbf{A}) = \{x \mid x = \mathbf{A}s \mod q \text{ for some } s \in \mathbb{Z}_q^l\} \subseteq \mathbb{Z}_q^m$$
. Then the expected number of lattice points inside  $C_\epsilon$  is 
$$\mathbb{E}_{\mathbf{A}}[\#(\mathcal{L} \cap C_\epsilon)] = \mathbb{E}_{\mathbf{A}}[\sum_{v \in \mathcal{L}} 1(v \in C_\epsilon)]$$

$$= \sum_{v \in \mathcal{L}} \mathbb{E}_{\mathbf{A}}[1(v \in C_\epsilon)] = \sum_{v \in \mathcal{L}} \Pr[v \in C_\epsilon]$$

$$= \sum_{v \in \mathcal{L} \cap [-R, R]^m} \Pr[v \in C_\epsilon] = p \cdot \#(\mathcal{L} \cap [-R, R]^m) \text{ where}$$
the fourth equality is by  $\Pr[v \in C_\epsilon] = 0 \text{ for } v \notin [-R, R]^m$ 

the fourth equality is by  $\Pr[v \in C_{\epsilon}] = 0$  for  $v \notin [-R, R]^m$ . By Minkowski's Convex Body Theorem,  $\frac{\operatorname{vol}(S)}{\det(\mathcal{L})}$  esti-

mates the number of lattice points in set S [74]. Let S be

 $B_m(R)$ , the m-dim. sphere of radius R inscribed within the  $[-R,R]^m$ . Then for a random lattice  $\mathcal{L}(\mathbf{A})$  where  $\mathbf{A}$  is full rank, the number of lattice points in  $B_m(R)$  is

$$\mathbb{E}[\#(\mathcal{L} \cap B_m(R))] = \frac{\text{vol}(B_m(R))}{\det(\mathcal{L})} = R^m \frac{\text{vol}(B_m(1))}{\det(\mathcal{L})} = R^m \frac{\text{vol}(B_m(1))}{q^{m-l}} = R^m \frac{\pi^{m/2}/(m/2)!}{q^{m-l}} \approx R^m \frac{(2\pi e/m)^{m/2}}{q^{m-l}}.$$
(3)

The third equality holds because  $det(\mathcal{L}(\mathbf{A})) = q^{m-l}$  for a full-rank matrix A, and the last  $\approx$  is by Stirling's approximation. By Lemma 4.4 of [68], A is full rank with probability at least  $1 - 1/q^{m-l}$  as needed in the Theorem.

Define  $\lambda_1$  to be the largest radius such that  $\mathbb{E}[\#(\mathcal{L} \cap$  $B_m(\lambda_1))] = 1$ . If we set  $R = \lambda_1$  in Eqn (3), we can get the expression  $\mathbb{E}[\lambda_1] = \sqrt{\frac{m}{2\pi e}}q^{1-l/m}$ . Now consider setting  $R \geq \alpha \mathbb{E}[\lambda_1]$ . By Eqn (3),  $\mathbb{E}[\#(\mathcal{L} \cap B_m(R))] \geq \mathbb{E}[\#(\mathcal{L}, B_m(\alpha \mathbb{E}[\lambda_1]))] = (\alpha \mathbb{E}[\lambda_1])^m \frac{(2\pi e/m)^{m/2}}{q^{m-l}} = \alpha^m$ . Then for  $C_{\epsilon} \subset [-R, R]^m$  (see Definition 9), we get

$$\mathbb{E}[\#(\mathcal{L} \cap C_{\epsilon})] \ge p \cdot \alpha^m = \frac{2^{h+m\log(\alpha)}}{(2R+1)^m}$$
 (4)

where the inequality and equality are directly by Fact 1.

We take log on both sides of Eqn (4), and set  $\gamma =$  $\log\left(\frac{2^{h+m\log(\alpha)}}{(2R+1)^m}\right) = h + m\log(\alpha) - m\log(2R+1)$  as in Theorem statement. So, we get **Fact 2**:  $\mathbb{E}_{\mathbf{A}}[\#(\mathcal{L}\cap C_{\epsilon})] \geq 2^{\gamma}$ .

Fix an arbitrary y according to Theorem 12. Notice that any result for  $C_{\epsilon}$  also holds for a shifted  $C_{\epsilon} - \mathbf{y}$  because the result is derived independently of the choice of C. Fact 2 also holds for  $\mathbb{E}_{\mathbf{A}}[\#(\mathcal{L}\cap(C_{\epsilon}-\mathbf{y}))] \geq 2^{\gamma}$ . This is equivalent to  $\mathbb{E}_{\mathbf{A}}[\#\mathbf{b} \in \mathbb{Z}_q^l \text{ s.t. } -\mathbf{A}\mathbf{b} = \mathbf{x} - \mathbf{y} \text{ for some } \mathbf{x} \in C_{\epsilon}] = \mathbb{E}_{\mathbf{A}}[\#\mathbf{b} \in \mathbb{Z}_q^l \text{ s.t. } \mathbf{y} - \mathbf{A}\mathbf{b} = \text{ for some } \mathbf{x} \in C_{\epsilon}] \geq 2^{\gamma}$ . So by Definition 10, y is  $2^{\gamma}$ -ambiguous for A on expectation. Then by Lemma 4,

$$\mathbb{E}_{\mathbf{A}} \max_{\mathbf{b}} \Pr[\mathbf{b} | \mathbf{A}\mathbf{b} + \mathbf{x} = \mathbf{y}] \le 2^{-\gamma}.$$
 (5)

Since y is arbitrary, Eqn (5) holds for all By Definition 11,  $H_{\infty}(\mathbf{b}|\mathbf{Ab} + \mathbf{x})$  $-\log(\mathbb{E}_{\mathbf{A},\mathbf{y}} \max_{\mathbf{b}} \Pr[\mathbf{b}|\mathbf{A}\mathbf{b} + \mathbf{x}] =$  $\mathbf{y}])$  $\geq -\log(2^{-\gamma}) = \gamma.$ 

**Lemma 2.** Let  $\beta \in \mathbb{Z}, m \in 2\mathbb{Z}, \epsilon \in \mathbb{R} > 0$ . Then  $C_{\epsilon} \subseteq \mathbb{R}$  $[-R,R]^m$  satisfies  $f(\beta,\epsilon,m):=|C_\epsilon|=\beta\cdot \frac{\pi^{m/2}}{(m/2)!}\epsilon^m$ .

*Proof.* The volume of  $B_m(\epsilon)$  is  $\operatorname{vol}(B_m(\epsilon)) = \frac{\pi^{m/2}}{\Gamma(m/2+1)} \epsilon^m$ , or simply  $\operatorname{vol}(B_m(\epsilon)) = \frac{\pi^{m/2}}{(m/2)!} \epsilon^m$  for even  $m^9$ . Then  $|C_\epsilon| = \beta \cdot \operatorname{vol}(B_m(\epsilon)) = \beta \cdot \frac{\pi^{m/2}}{(m/2)!} \epsilon^m$  by Definition 9.  $\square$ 

**Lemma 3.** For  $\mathcal{X} = \mathcal{U}(C_{\epsilon})$ ,  $H_{\infty}(\mathcal{X}) = \log(f(\beta, \epsilon, m))$ .

*Proof.* By Definition 11,  $H_{\infty}(\mathcal{X}) = H_{\infty}(\mathcal{U}(C_{\epsilon})) =$  $-\log(\max \Pr[\mathcal{U}(C_{\epsilon})]) = -\log\left(\frac{1}{|C_{\epsilon}|}\right)$ . By Lemma 2  $H_{\infty}(\mathcal{X}) = \frac{1}{f(\beta \in m)} = \log(f(\beta, \epsilon, m)).$ 

9. As m is typically even in practice, we assume so henceforth.

**Lemma 4.** Fix a matrix  $\mathbf{A} \in \mathbb{Z}_q^{m \times l}$ . Let  $\mathbf{y} \in \mathbb{Z}_q^m$  be  $2^{\gamma}$ -ambiguous for the matrix  $\mathbf{A}$  and error distribution  $\mathcal{X} = \mathcal{U}(C_{\epsilon})$ . Let  $\mathbf{b} \leftarrow \mathcal{U}(\mathbb{Z}_q^l)$  and  $\mathbf{x} \leftarrow \mathcal{X}$ . Then for all  $\mathbf{z} \in \mathbb{Z}_q^l$ ,

$$\Pr[\mathbf{b} = \mathbf{z} | \mathbf{A} \mathbf{b} + \mathbf{x} = \mathbf{y}] \le 2^{-\gamma}.$$

In other words,  $\max_{\mathbf{b}} \Pr[\mathbf{b}|\mathbf{Ab} + \mathbf{x} = \mathbf{y}] \leq 2^{-\gamma}$ .

The proof is similar to that of Lemma 4 in [52], since  $\mathcal{X}$  is also a uniform distribution over its support.

*Proof.* Since **b** and **x** are drawn from uniform distributions,  $p := Pr[\mathbf{b} = \tilde{\mathbf{b}}, \mathbf{x} = \tilde{\mathbf{x}}]$  is the same for all  $\tilde{\mathbf{b}} \in \mathbb{Z}_q^l$  and  $\tilde{\mathbf{x}} \in \mathcal{X}$ . Let  $S := \{\mathbf{z} \in \mathbb{Z}_q^l | \mathbf{y} - \mathbf{A}\mathbf{z} \in \operatorname{supp}(\mathcal{X})\}$ . As  $\mathbf{y}$  is  $2^{\gamma}$ -ambiguous it holds that  $|S| \geq 2^{\gamma}$ , thus

$$\begin{split} Pr[\mathbf{A}\mathbf{b} + \mathbf{x} &= \mathbf{y}] = \sum_{\mathbf{z} \in \mathbb{Z}_q^n} Pr[\mathbf{A}\mathbf{b} + \mathbf{x} = \mathbf{y}, \mathbf{b} = \mathbf{z}] \\ &= \sum_{\mathbf{z} \in S} Pr[\mathbf{x} = \mathbf{y} - \mathbf{A}\mathbf{z}, \mathbf{b} = \mathbf{z}] \geq p \cdot 2^{\gamma}. \end{split}$$

Thus it holds for all  $\mathbf{z} \in \mathbb{Z}_q^n$  that

$$Pr[\mathbf{b} = \mathbf{z} | \mathbf{A}\mathbf{b} + \mathbf{x} = \mathbf{y}] = \frac{Pr[\mathbf{b} = \mathbf{z}, \mathbf{A}\mathbf{b} + \mathbf{x} = \mathbf{y}]}{Pr[\mathbf{A}\mathbf{b} + \mathbf{x} = \mathbf{y}]} \le \frac{1}{2^{\gamma}}.$$

# **B.3. Proof of L2FE-Hash Security**

**Proof of Theorem 1.** Let D denote the procedure in Algo. 3 of obtaining a d=(A,Ab+x) value from  $x \overset{\mathcal{X}}{\leftarrow} C_{\epsilon}$ . From Theorem 12, we know that  $\tilde{H}_{\infty}(X|D(X)) \geq \gamma$ . Note that  $\tilde{H}_{\infty}(B|D(X))$  is the same value because for fixed A,Ab+x, there is a 1-to-1 correspondence between b and x. Notice that  $b \in \mathbb{Z}_q^l$  is a  $l\log(q)$ -bit string. Since Ext is an average case  $(l\log(q),\gamma,\kappa,\epsilon_{\mathrm{FE}})$ -strong extractor, then by Definition 7, applying this strong extractor to b gives  $\mathrm{SD}((\mathrm{Ext}(B,K),D(X),K),(\mathcal{U}(\{0,1\}^\kappa),D(X),K)) = \mathrm{SD}((R,P),(\mathcal{U}(\{0,1\}^\kappa),P)) \leq \epsilon_{\mathrm{FE}}.$ 

Since Ext can extract  $\kappa \le \gamma - 2\log(1/\epsilon_{\rm FE}) + 2$  bits of randomness by Lemma 2.4 of [25], the proof completes.  $\Box$ 

# Appendix C.

# FE Implements the Ideal Primitive

We formally prove Theorem 2 in this section, that a computationally secure FE achieves all the properties required by an ideal primitive. The formal definition of the entropy notion in the utility property is given in Definition 13.

**Definition 13** (HILL Entropy [73]). Let X be a random variable. X has  $\epsilon$ -HILL computational entropy  $H^{HILL}_{\epsilon}(X)$  at least  $\kappa$  if there exists a random variable Y such that  $\tilde{H}_{\infty}(Y) \geq \kappa$  and  $X \stackrel{comp}{\approx_{\epsilon}} Y$ .

**Proof of Theorem 2. Correctness proof.** The correctness property of the ideal primitive is the same as that of FE.

**Algorithm 4** Construction of A with A'.

1: Input: (r, p)2: x' := A'(r, p)

- 3: r' := Rep(x', p)
- 4: If r' = r, then return b' := 1, else return b' := 0.

**Utility proof.** The FE security property implies a utility argument that translates to the utility property Prop. 3 of the ideal primitive.

Since  $H_{\infty}(\mathcal{U}(\{0,1\}^{\kappa}),\mathcal{P})=H_{\infty}(\mathcal{U}(\{0,1\}^{\kappa}))=\kappa$ , and  $(\mathcal{R},\mathcal{P})\approx_{\epsilon_{\mathrm{FE}}}(\mathcal{U}(\{0,1\}^{\kappa}),P)$  by FE security, then  $H^{\mathrm{HILL}}(\mathcal{R},P)\geq\kappa$  by Definition 13.

**Security proof.** To prove that FE security implies ideal primitive security, we first describe the FE and ideal primitive security games below. Subscripts on adversaries annotate the data utilized by them. The knowledge of input distribution  $\mathcal{X}$  is assumed to be accessible to all adversaries.

Game  $G_0$  (FE security game):

- Challenger C flips a bit  $b \leftarrow U(\{0,1\})$ .
  - If b=1,  $\mathcal C$  samples  $x\leftarrow \mathcal X$ , and computes  $(r,p)=\operatorname{GEN}(x)$ .
  - If b = 0, C samples  $x \leftarrow \mathcal{X}$ , computes  $(\_, p) = \text{GEN}(x)$ , and samples  $r \leftarrow \mathcal{U}(\{0, 1\}^{\kappa})$ .
- Adversary  $\mathcal{A}$  receives (r,p) and outputs a guess b'. The game  $G_0$  outputs 1 if b'=b. Advantage of  $\mathcal{A}$  is defined as

$$Adv_0(A) = |\Pr[A_{(r,p,X)} = 1 \mid b = 1] - \Pr[A_{(p,X)} = 1 \mid b = 0]|.$$

Game  $G_1$  (Ideal primitive security game):

- Challenger  $\mathcal{C}$  samples  $x \leftarrow \mathcal{X}$  and computes  $(r, p) = \operatorname{GEN}(x)$ .
- Adversary  $\mathcal{A}'$  receives (r,p) and outputs a guess x'.

The game  $G_1$  outputs 1 if  $d(x, x') \leq t$ . Advantage of  $\mathcal{A}$  is

$$\mathrm{Adv}_1(\mathcal{A}') = \left| \Pr[G_1(\mathcal{A}'_{(r,p,\mathcal{X})}) = 1] - \Pr[G_1(\mathcal{A}'_{(p,\mathcal{X})}) = 1] \right|.$$

Game  $G_0$  directly reduces to  $G_1$  as shown in Algo. 4. In particular, the probability of  $\mathcal A$  returning 1 in either b=0 or b=1 case depends on the success probability of  $\mathcal A'$  in recovering x' and the correctness of REP procedure. Therefore, we can derive  $\mathrm{Adv}_0(\mathcal A)=(1-\delta)\mathrm{Adv}_1(\mathcal A')$ :

$$\begin{aligned} \operatorname{Adv}_{0}(\mathcal{A}) &= \left| \operatorname{Pr}[\mathcal{A}_{(r,p,\mathcal{X})} = 1 \mid b = 1] - \operatorname{Pr}[\mathcal{A}_{(p,\mathcal{X})} = 1 \mid b = 0] \right| \\ &= \left| \operatorname{Pr}[G_{1}(\mathcal{A}'_{(r,p,\mathcal{X})}) = 1] - \operatorname{Pr}[G_{1}(\mathcal{A}'_{(p,\mathcal{X})}) = 1] \right| \\ &\cdot \operatorname{Pr}[\operatorname{REP} \text{ is correct}] \\ &= (1 - \delta)\operatorname{Adv}_{1}(\mathcal{A}') \end{aligned}$$

So  $\epsilon_{\mathrm{FE}}\text{-FE}$  security implies  $\epsilon_{\mathrm{FE}}(1-\delta)$ -ideal primitive security

# Appendix D. Prior Attacks Details

**Attack details.** Bob attack uses an ID loss function which requires information about the feature extractor, hence making the attack whitebox [14]. Bob's inversion model uses

special blocks in its architecture called DSCasConv which are cascaded convolutions with skip connections.

GMI first trains a GAN model to learn the mapping between a latent space and the image data, then during the attack phase, uses the discriminator feedback and target model classification to optimize the latent vector corresponding to each user. KED-MI improves upon GMI by using the target model's output labels in training of the GAN model, resulting in target-model specific attack models.

Implementation details. For GMI and KED-MI attacks, we use the same attack pipeline as [15]. For GMI, we use their pretrained GAN model, and for KED-MI, we train our own GAN model for each target model. In particular, 1000 users were chosen to train the classification layer, with around 27 images per user in the train set, and 3 images per user in the test set. 30,000 images of 6453 users different from those 1000 chosen were used to train the KED-MI GAN model. For Bob, we use only one image per user to train the inversion model, for all 9177 users in our Celeb-A train set, without data augmentation.

To customize the attacks for target models with different protection schemes, we use the same model architecture as the facenet-pytorch model [75], and append a final layer that generates protection scheme outputs from the FaceNet embeddings. For example, the final layer returns Rx||R.flatten() for the MRP protection scheme, ss for Facial-FE, and Ab+x||A.flatten() for L2FE-Hash.

# Appendix E. Supplementary Results

We evaluate the quality and similarity of reconstructed images to the original images by computing the Learned Perceptual Image Patch Similarity (LPIPS) metric [9] and the Fréchet inception distance (FID) metric [48]. We claim that LPIPS is no different from PIPE ASR when using a different face recognition model during evaluation than the one used during training. Hence, we also evaluate PIPE ASR across 3 different feature extractor models. All images are resized to  $64 \times 64$  before evaluation.

LPIPS score. LPIPS is a perceptual similarity metric developed as a proxy to human perception. It relies on the closeness of features obtained from a deep learning model. As seen in Table 8, we observe two trends. First, we see that PIPE has a smaller score than Bob on average, indicating that PIPE reconstructed images are closer to the originals than Bob. Second, there is a sharp increase in the LPIPS score for L2FE-Hash. This is because while the reconstructed faces are close to human faces, they are not similar to the original face, indicating that L2FE-Hash is a successful defense.

**FID score.** FID scores assess the quality of reconstructed images by comparing the distance between the reconstructed and original image distributions. We use the PyTorch-FID library implementation [76]. As seen in Table 9, FID score for PIPE is much lower than that of Bob, indicating that the distribution of images reconstructed using PIPE is of

TABLE 13: Cross model ASR (in %) of PIPE, trained and evaluated on the Celeb-A dataset. Column headings indicate the model used for evaluation.

Model	Scheme	Facenet	ArcFace	VGG-Face
Facenet	Unprotected	-	89.8	98.8
	Facial-FE		87.8	97.8
	MRP		76.1	88.2
	L2FE-Hash		5.7	1.4
Arcface	Unprotected	93.1 90.2 36.7 1.1	-	95.4
	Facial-FE			91.3
	MRP			41.8
	L2FE-Hash			1.7

similar quality to that of original images. It is worth noting that the FID score increases significantly for Bob with MRP and L2FE-Hash protection schemes, unlike PIPE. This is because Bob is not able to produce good-quality face images given these embeddings, whereas PIPE still produces human-looking images that are not close to the original images. Hence, FID does not capture the privacy risk.

Cross-model PIPE ASR. Since LPIPS relies on closeness of deep embeddings, we believe that PIPE ASR computed using a feature extractor different from the one used by the target model also represents a similarity metric. We use Facenet, ArcFace, and VGG-Face [77] as feature extractors on the Celeb-A dataset to compute ASR. Table 13 shows that the reconstructed images are still considered t-close to the original images and successfully authenticate with ASR  $\geq 76\%$  in most cases. Therefore, the PIPE cross-model ASR is indicative of the performance we would expect from any other ML-based similarity metric like LPIPS.